PHYSICAL PROPERTIES OF SELECTED SCORIA CONES IN NEW MEXICO

by

Jo Anne Cima

Submitted in Partial Fulfillment
of the Requirements for the Degree of
Master of Science in Geology

New Mexico Institute of Mining and Technology

Socorro, New Mexico

December 1978

ABSTRACT

Examination of four dissected scoria cones in New Mexico reveals a predictability in the color, sorting, and grain size of the tephra. The four cones, which are located in three widely separated parts of the state, all have a vent-centered, concentric color pattern. The tephra is dark red-brown near the vent, dark grey with iridescent surface coatings at intermediate distances, and very dark-grey with no surface iridescence near the perimeter. Chemical analysis of samples indicate that these color patterns reflect a gradual increase in the amount of ferric iron to total iron toward the vent. Laboratory heating tests suggest that this oxidation can be caused by increased temperature; perhaps related to the vent. The iridescence coatings are apparently due to partial oxidation of the iron and can be reproduced by heating scoria fragments in the laboratory. Average grain size decreases consistently away from the vent. Sorting is commonly moderate and varies inversely with medium grain size within a scoria cone.

The predictability of physical properties of scoria cones is indeed important in their exploitation by the construction and landscaping industries. Such information would allow companies to develop pits with more assurance of the color and quality than before.

TABLE OF CONTENTS

LIST OF FIGURES

LIST OF TABLES

LIST OF APPENDICES

ACKNOWLEDGEMENTS

Many people contributed their time and help to me during this study; I wish to offer them my sincere thanks. The operators of the scoria operations, Leroy Ellis and Carroll Morton and their staffs, generously allowed me to study their scoria deposits. These men spent many hours answering my questions and giving me physical support in the field. Lynn Brandvold taught me many of the chemical procedures used during this study. Bob Osburn took many of my photographs and polished both my writing style and my drafted figures. Dr. Clay T. Smith and Dr. Frederick J. Kuellmer both critically read my manuscript as well as served as members of my thesis committee.

The study was funded mainly by the New Mexico Bureau of Mines and Mineral Resources. The Bureau provided a graduate research assistantship, the use of chemicals and atomic absorption spectrometry equipment, and of microscopes. The Scientific Research Society of North America (Sigma Xi) provided me with a grant to cover the cost of photographs and physically produce this manuscript.

A special thanks is extended to Dr. George Austin.

He reviewed many drafts of my manuscript and offered many criticisms and suggestions.

INTRODUCTION

Volcanic landforms, including scoria cones, have been observed by mankind since ancient time. The association of volcanic events with landform-building processes, however, was not made until the late eighteenth century by Hutton and Lyell (Bullard, 1962).

The nomenclature used to describe extrusive volcanic rocks has not been standarized. Some of the nomenclature systems currently used are illustrated in Table 1. The terms "ash" and "cinders" were first applied to pyroclastics because the materials resemble ash and cinders from fireplaces (Bullard, 1962). Recent investigators (Porter, 1972; Francis and Thorpe, 1974) use the term "scoria" to replace "cinder". At various times, pyroclastic cones have been called scoria mounds, most commonly, cinder cones, and recently, scoria cones. I have used the terms "scoria" and "scoria cones" because they are in current usage and, more importantly, because they describe the texture of the material making up a scoria deposit. Rittman's (1962) size classification scheme and Walker and Croasdale's (1971) textural terms are used in this report. "Tephra" is used, in this study, synonymously with "pyroclastic materials" following the convention of Thorarinsson (1954).

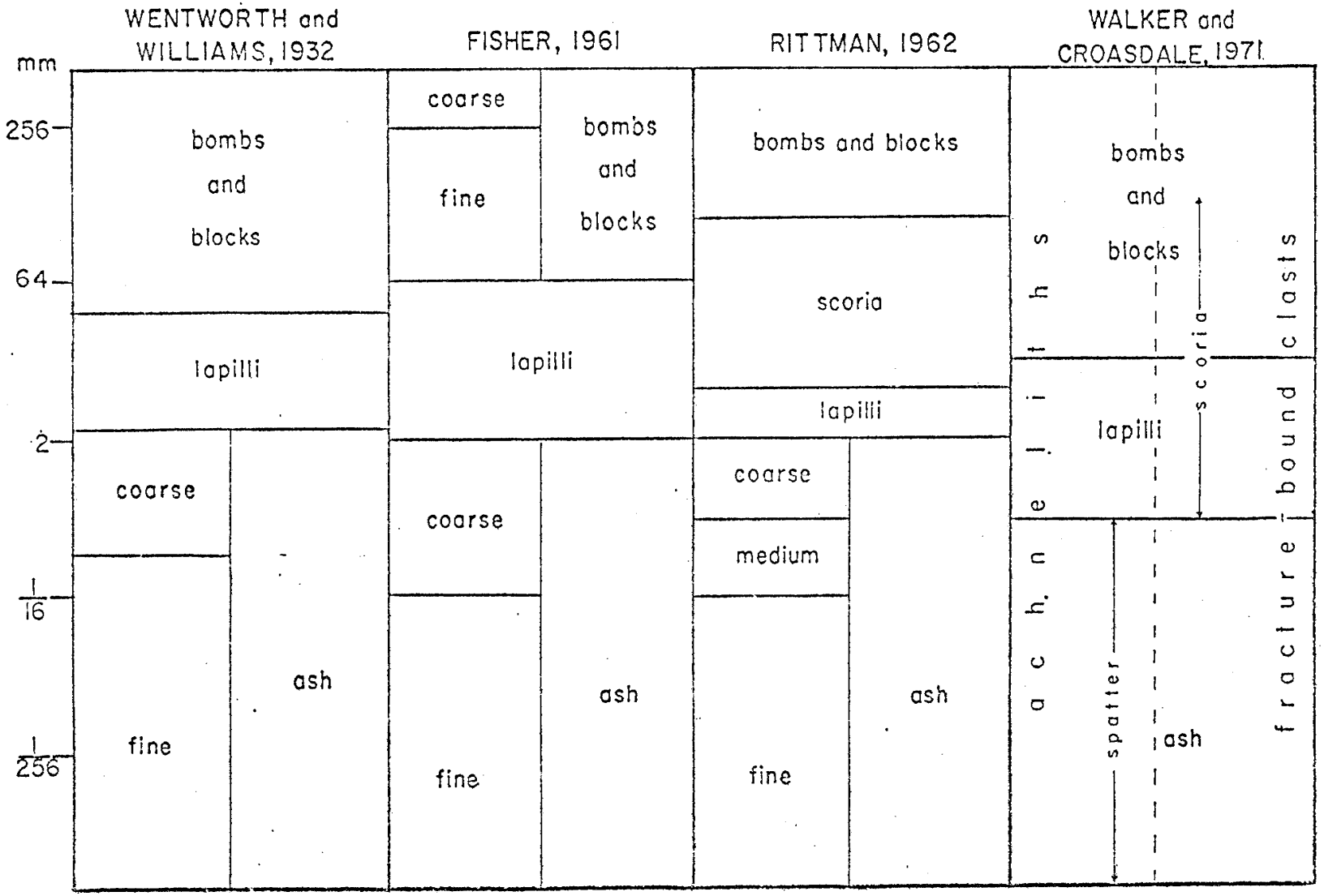

Table 1: Classification systems of extrusive volcanic rocks currently in use by the majority of workers.

Scoria cones are produced when volatiles, coarse fragments, and molten magma are ejected from a conduit and build a roughly conical landform around the vent (Macdonald, 1967). The cone grows as successive showers of tephra mantle the developing cone. For this reason, cones can be studied as a type of sedimentary accumulation.

Scoria cones are common products of minor basaltic acitivity on land often built late in the eruptive history of a vent (Porter, 1972). The cone can be built by a single eruption or by episodic eruptions, with or without lengthy inactive periods between eruptions (Wilcox, 1959). Scoria cones examined in Mexico, Arizona, and Hawaii have been shown to be composed of tephra having well-defined size, shape, and lithologic characteristics (Walker and Croasdale, 1971). Variations in the size and general morphology of scoria cones are determined largely by a set of variables that describe certain natural conditions and processes:

1. Force and duration of eruption
2. Angle at which the tephra is ejected
3. Wind directions and speed
4. Quantity and size distribution of tephra
5. Density of the material and subsequent angle of repose and volume occupied
6. Original topography covered by the deposit.

PURPOSE AND SCOPE

The purpose of this investigation is to study the physical and stratigraphic characteristics of the tephra making up selected scoria cones in New Mexico. Physical characteristics of the tephra examined include:

1. Size, shape, and general appearance of the tephra in and around a scoria cone
2. Correlation of individual sedimentation units with events in the eruptive history
3. The relationship of color variations on the cone to the variations of the oxidation state of iron.

The characteristics of each scoria cone are considered separately. Common trends in the study cones can then be evaluated with respect to geological significance and the economic potential of the scoria cones.

METHODS

Some 75 scoria cones in New Mexico, both quarried and unexploited types, were examined during a systematic field and map reconaissance (Fig. 1). From these, four cones were selected for detailed study. Partially dissected cones were chosen, allowing observation of internal stratification as well as the appearance of the tephra in place. Internal features present in the study cones were compared with other scoria cones in New Mexico and some described in the literature from Hawaii, Arizona and Iceland.

Grain size characteristics of samples taken from the study cones were examined using a binocular microscope. In addition, selected samples were sieved to compare position in the cone to median grain size and degree of sorting. The variation of the oxidation state of iron within each deposit was determined by using standard atomic absorption spectrometry and gravimetric techniques. Heating tests were conducted to determine the range of temperature in the laboratory required to reproduce the oxidation patterns of iron observed in the field.

Sample colors were measured by comparison with the Munsell Soil Color Chart. The Munsell notation for color consists of separate notations for hue, value, and chroma

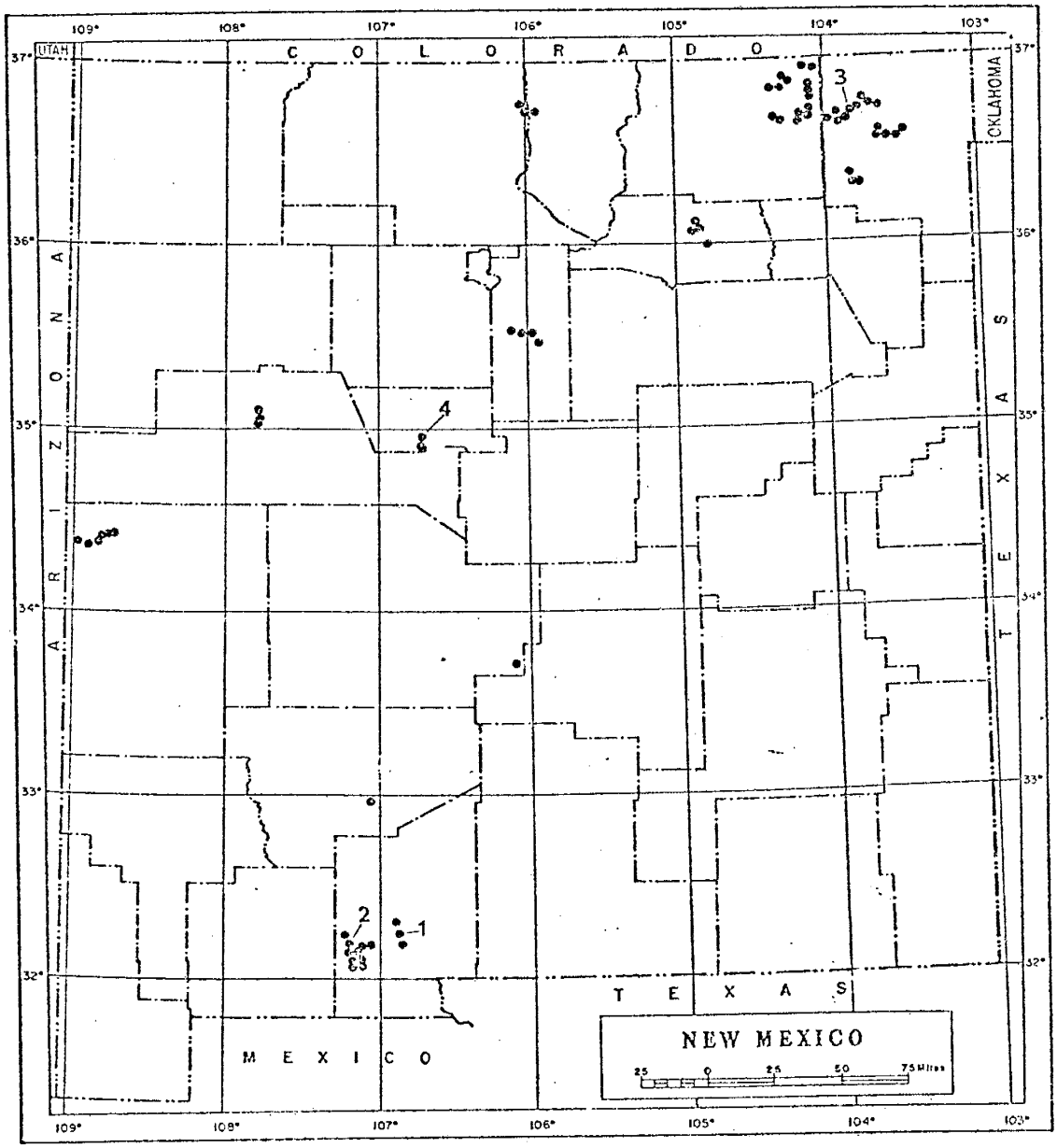

Figure 1: Distribution of scoria cones in New Mexico examined as an early part of this study. Numbers correspond to the study cones as follows: 1 - Santo Tomas Mountain, 2 - Aden Cone, 3 - Twin Mountain, and 4 - Blackbird Hill.

which are combined in that order to form the color designation. For example, the Munsell notation of a color with a hue of 10R, a value of 5, and hue of 3 is 10R 5/3. The Munsell system uses a color name to complete the color description which, in this case, is a weak red. Both the color name and the Munsell notation are used in this report. A more complete explanation of the use of the Munsell Soil Color System is found in Appendix 1.

The study cones have been divided into three, somewhat subjective, roughly concentric zones around the vent. For the purpose of discussion, these zones will be defined as follows:

> Vent Zone: Area at the vent to the point where the slope of tephra beds changes from inward-dipping to outward dipping. Tephra coloration varies from weak red to dark reddish-brown. Sorting is generally poor.
>
> Intermediate Zone: Area from the edge of the vent zone to a point where there is no surface iridescence on scoria fragments. Material in this region is moderately sorted and of a variety of colors. This zone interfingers with the perimeter zone.
>
> Perimeter Zone: Area farthest from the vent, characterized by uniform, very dark-grey color and a high degree of sorting.

PREVIOUS INVESTIGATIONS

Scoria cones are commonly discussed as small portions of broad treatises on shield volcanoes or basaltic flows; seldom are cones studied independantly. A large data base on extrusive volcanic rocks exists and much general information on pyroclastic deposits and volcanic geomorphology can be utilized in the study of scoria cones.

Classifications systems have been devised for the several types of volcanoes, eruptions, and pyroclastic materials. Colton (1937) developed a classification for scoria cones in the San Francisco volcanic field of northern Arizona based on erosional characteristics. Later work in this area by Breed (1964) added crater morphology to Colton's original classification scheme. Cotton (1944) subdivided volcanoes into basalt cones, shield cones, composite cones, and scoria cones.

Recent workers have compared scoria cones to other volcanic features, such as maars, on a semi-quantitative basis. Ward (1973) developed a deterministic (mathematical) model of pyroclastic deposition. Other workers have examined the differences between the products of Strombolian-type and Surtseyan-type volcanism. Definitive characteristics

include: variation in tephra (Walker and Croasdale, 1971), variations in the lithology and external morphology of the cones (Francis and Thorpe, 1974), and variation in aspect ratio, which is defined as the ratio of cone height to basal diameter (Porter, 1972; Green, 1975). Each parameter exhibits specific trends for Surtesyan verses Strombolian-type eruptions.

STUDY CONES

Santo Tomas Mountain

Location and Access

Santo Tomas Mountain scoria cone (Fig. 2) is located in the Potrillo volcanic field 9 miles south of Las Cruces, New Mexico, and one mile west of the Rio Grande Valley (SW 4, sec. 31, T. 24S., R. 2E.). Seven miles south of La Mesilla (a suburb of Las Cruces) a dirt road owned by Stahman Farms leads west to the cone from New Mexico Highway 28 (Fig. 2). Black arrows mark the haulage route to the cone through a maze of orchard roads. The deposit has been actively quarried since 1972, providing materials to use in the manufacture of lightweight cinder blocks and as roofing chips and landscape material.

Physiographic Setting

Santo Tomas Mountain lies within the Mesilla Bolson which lies within the intermontane basin region northeast of the Sierra Madre Occidential (Hawley, 1969). The Sierra Madre is considered to be the southern extension of the Mexican Highlands section of the Basin and Range Province (Fenneman, 1931).

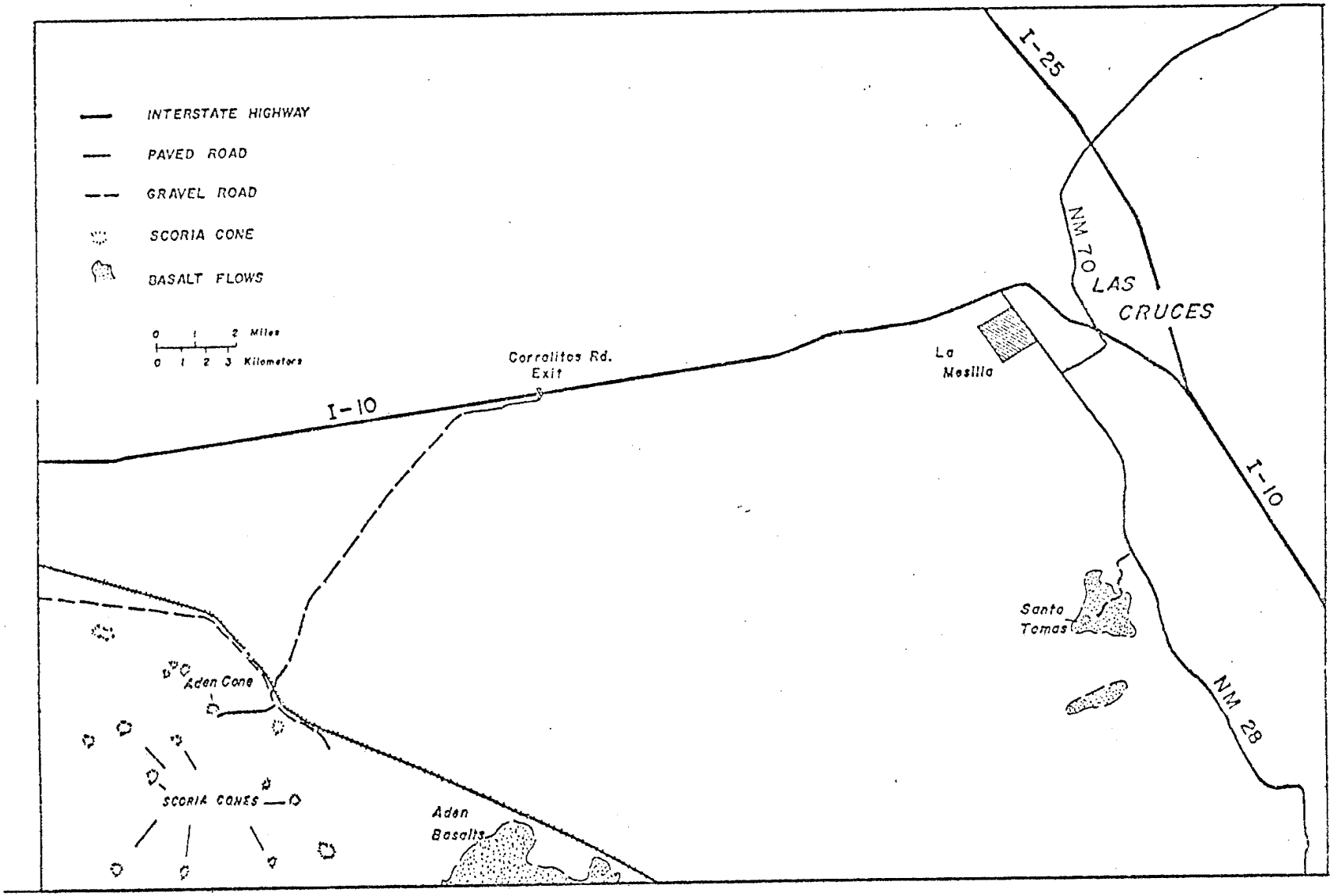

Figure 2: Location map of central Dona Ana county showing the locations of Santo Tomas Mountain and Aden Cone.

Geologic Environment

Santo Tomas Mountain is the northern-most of four volcanic centers (Fig. 3) aligned along the north-south trending Black Mountain-Santo Tomas fault (DeHon, 1965). Mineralogical and chemical similarities in all the flows of the Santo Tomas-Black Mountain basalts indicate an origin from a common magma source (Hoffer, 1971). Potassium-argon dating of the basalts suggest that the Santo Tomas eruptive center is the youngest of the four eruptive centers in the Santo Tomas-Black Mountain chain, erupting approximately 0.3 m.y. ago (Hoffer, 1973).

Santo Tomas Mountain is approximately 45 m high and has an average basal diameter of 310 m. The cone is nearly circular in map view and apparently erupted from one main vent. The bulk of the cone rests on the alkali olivine Santo Tomas basalt flows, thought by Hoffer (1969) to be nearly contemporaneous with the building of Santo Tomas Mountain. Age dates reported by Hoffer (1971) suggest that the formation of the scoria cone was a late-stage event in the eruptive history of the Santo Tomas center. The flows further north are older than those flows near the scoria cone (Fig. 4), suggesting a southern migration of the volcanic center.

The southwest section of the cone apparently built against an uneroded remnant of the rim of the La Mesa

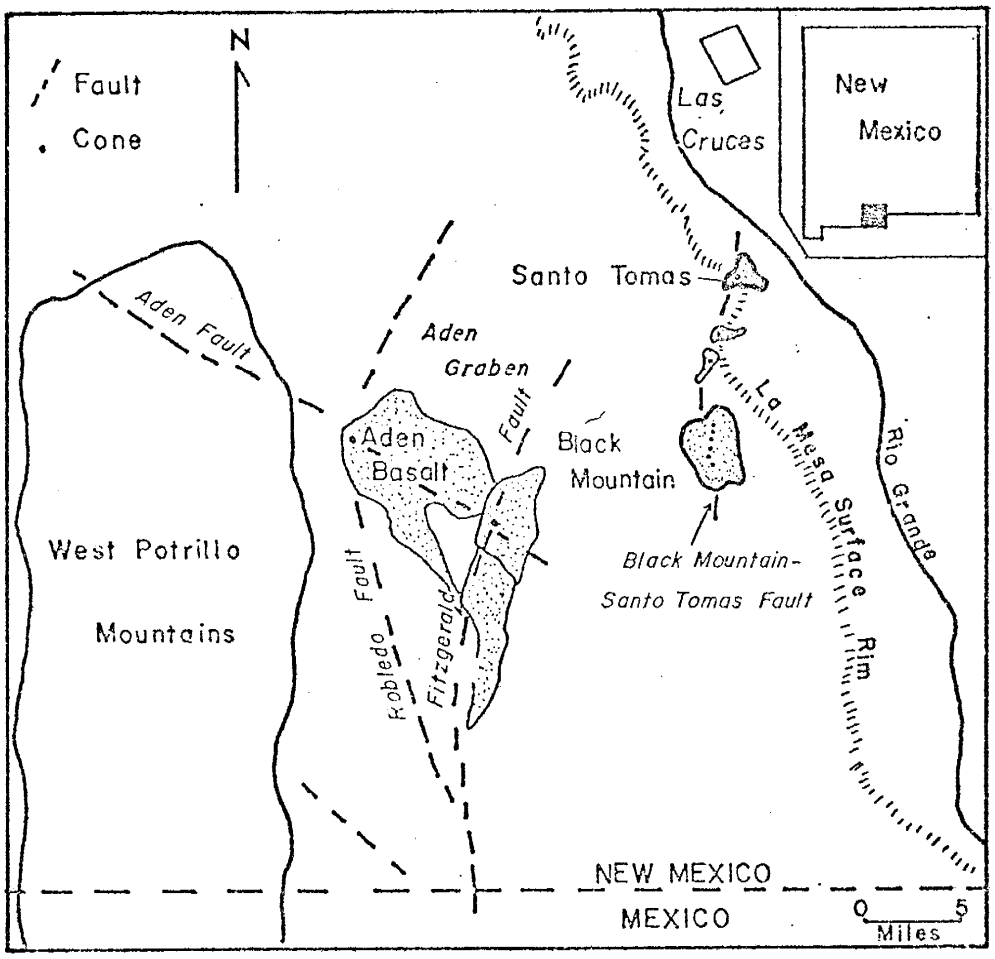

Figure 3: Index map of the Potrillo volcanic field (after Hoffer, 1973).

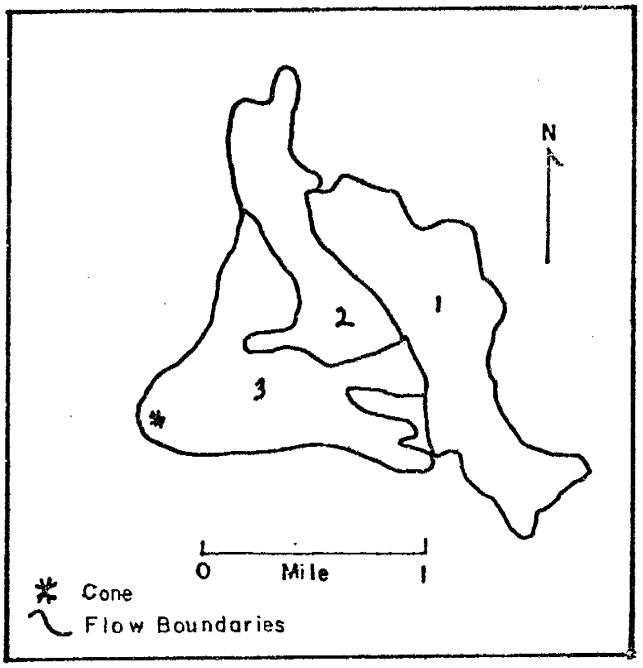

Figure 4: Santo Tomas Mountain and associated basalts numbered oldest (1) to youngest (3). (After Hoffer, 1969)

geomorphic surface (Hawley and Kottlowski, 1969). The growing cone mantled this uneroded remnant, thus preserving it for later exhumation during the excavation of the south side of the cone (Fig. 5). This remnant now appears as a 20 m sand bank containing stream-rounded pebbles up to 10 cm in diameter.

Pyroclastic Materials

Santo Tomas Mountain is composed of loose pyroclastic debris with smaller amounts of agglutinated tephra and rootless lava flows which are concentrated within 30 m of the vent (Fig. 6). The loose pyroclastic materials of the deposit are a combination of two textural types: fracture-bound clasts and achneliths (Walker and Croasdale, 1971). Fracture-bound clasts make up the bulk of the tephra in the lapilli to fine-bomb size range. These fragments are angular to subangular and are generally roughly equant in form (Fig. 7).

Achneliths (from the Greek "acne"-spray) make up as much as 50% of the coarse ash to lapilli size range. The shape of the achneliths is variable, however, most are elongate and have the appearance of frozen spatter (Fig. 8). The elongation of the achneliths has been attributed to stretching of the molten lava as it leaves the vent (Tsuya, 1941). Surface tension, gas content, and viscosity of the lava are thought to control this stretching (Walker and Croasdale, 1971).

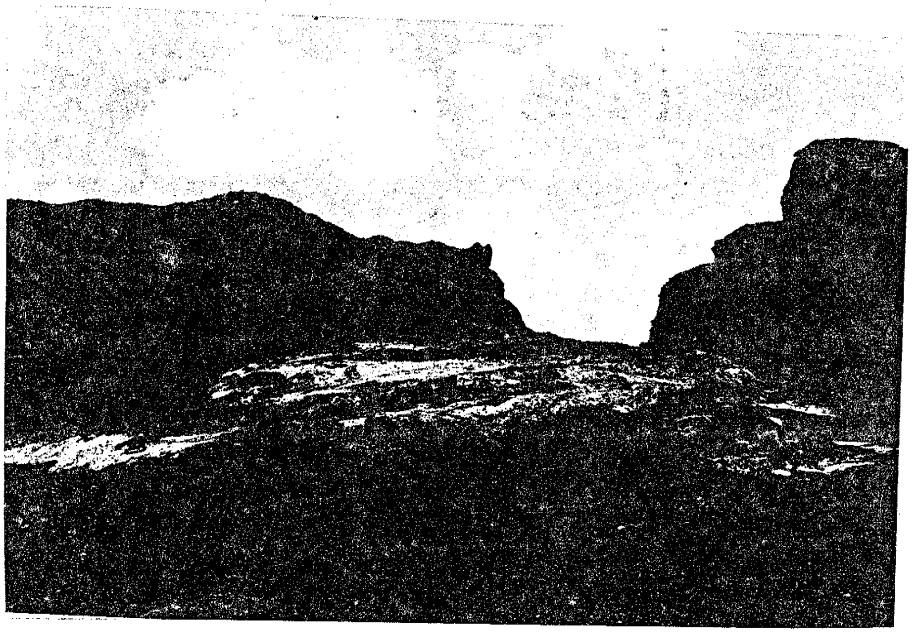

Figure 5: Cut in south side of Santo Tomas Mountain. Note light colored sand in midground, a remnant of the La Mesa Geomorphic surface. Cut in center of the photograph is fourteen meters across. Woman near cut is 1.58 m tall.

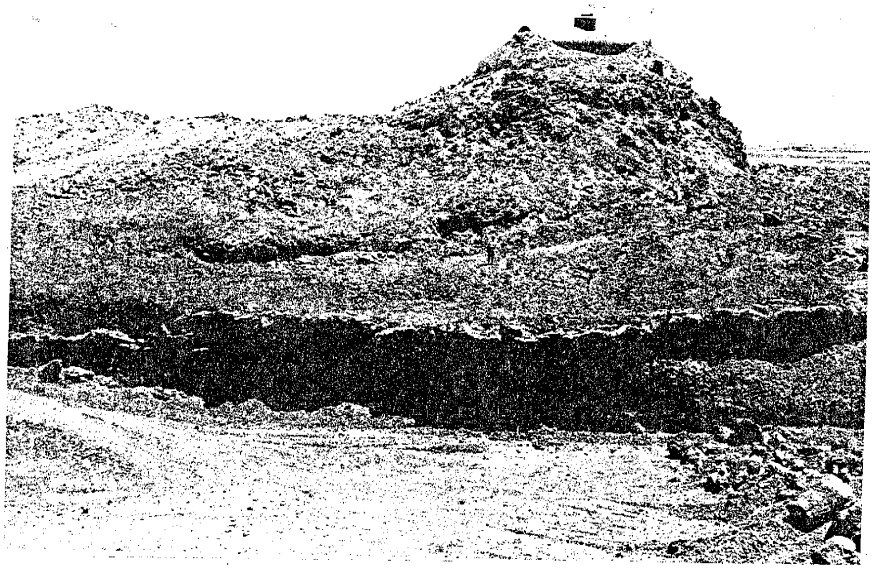

Figure 6: Lava flows dipping to the east and away from the vent at Santo Tomas Mountain. This photograph shows a large quarry in the vent area. It appears that the flow mantled the growing cone in all directions. Note the filled lava tube in the lower right corner. Water tank on the top of the hill is ten meters long. Woman at mid distance is 1.58 m tall.

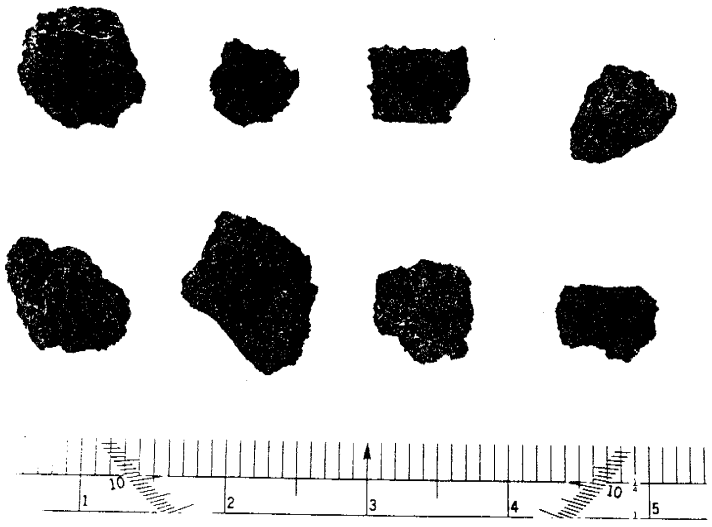

Figure 7: Fracture-bound clasts from Santo Tomas Mountain and Blackbird Hill showing generally equant form and fracture-bound surfaces.

Figure 8: Achneliths from Santo Tomas Mountain and Aden cone showing elongate form and glassy surfaces.

Poorly formed bombs and blocks are present in the cone, particularly in the lower portions of each sedimentation unit in the intermediate zone. The bombs are ragged in appearance, but still appear stretched out, resembling the achnelithic tephra present in the smaller sized clasts.

Many lava tubes, both drained and filled, are exposed in the lower portions of the cone (Fig. 6). The lava tubes are 1.2-1.8 m in diameter and passable for distances of 50 m in some cases. Lava stalactites are common on the roofs of the unfilled lava tubes. Similar features occur at Amboy Crater in California (Parker, 1963) and at Paricutin Volcano in Mexico (Bullard, 1962). The lava tubes have been attributed to late-stage, quiet outpourings of fluid lava from the central vent. Small lava driblets, 10-15 cm wide and 1-3 m long are common in the vent area of the cone (Fig. 9). Lava driblets assume their characteristic forms mainly from the forces of gravity and wind acting on the lava while still plastic (Wentworth and Williams, 1932).

The pyroclastic materials at Santo Tomas Mountain range from being well-stratified in the perimeter zone to unbedded in the vent zone. The tephra in the vent zone consists of dark red-grey (5R 3/1) agglutinate grading to loose scoria of the same color. Incipient

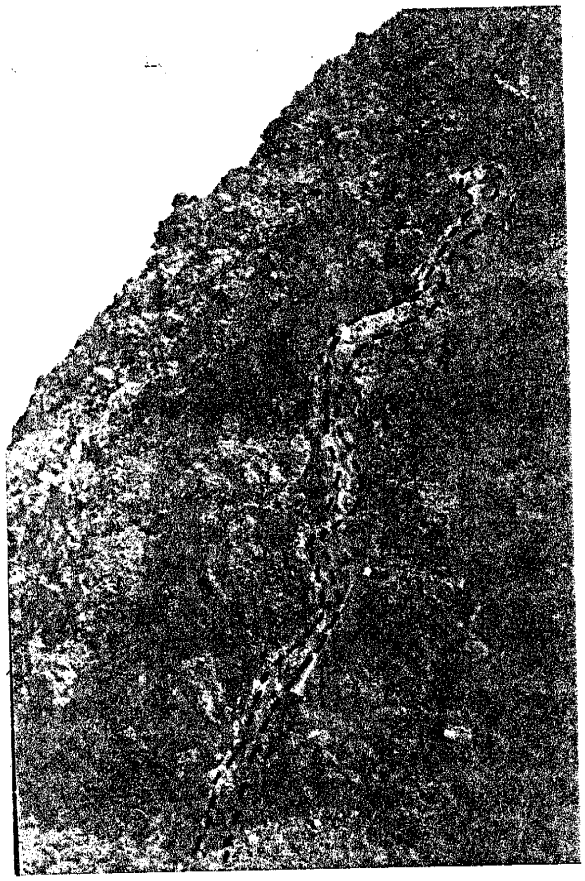

Figure 9: Lava driblet in center of photograph is exposed on the west side of Santo Tomas Mountain. This driblet is 10 cm wide and 2 m long. Hammer in lower center of picture is 33 cm long. Lava driblets are usually larger than lapilli size and assume their characteristic forms while plastic and chiefly as a result of forces acting at the time of detachment from the magma or at the time of landing after flight (Wentworth and Williams, 1932).

welding of the clasts has occurred, forming a well-consolidated volcanic breccia centered around the vent.

In the intermediate zone, 30-100 m from the vent, scoria is commonly very dark-grey (7.5YR N3/) and has some blue iridescent surface coatings. The beds in this interval commonly show a graded bedding within a 60-80 cm interval. The bottom of each layer is generally made up of large angular blocks and bombs mixed with scoria and lapilli. The upper sedimentation units are a uniform 2.5 cm lapilli size. This sequence appears to represent a sedimentation unit common in scoria cones. The bedding sequence suggests that an eruption pulse begins with the ejection of poorly sorted tephra from large block to coarse ash size. The blocks and bombs are probably derived from varied sources including material that fell back into the crater following the last eruption, angular fragments of agglutinate torn from the crater rim of the volcano, and exotic sedimentary fragments, mantled with scoriaceous material, from along the conduit walls (Fig. 10). As the eruption proceeds, the force of the eruption diminishes, producing material of relatively uniform texture and size. The material makes up the perimeter zone of Santo Tomas Mountain at distances greater than 100 m from the vent.

Figure 10: Cored bomb from Santo Tomas Mountain showing two layers of scoriaceous material. Core is a sedimentary fragment derived from the wall of the conduit. Bomb is approximately 10 cm long at the bottom of the photograph.

Eruptive History

Field evidence at Santo Tomas Mountain suggests that the cone was built by a series of eruptive events separated by short intervals of time. No erosion surfaces, soils, or dramatic changes in the characteristics of tephra are present to suggest longer periods of inactivity between eruption episodes. Thus, it is probable that Santo Tomas Mountain formed in a period of a few days to a few years.

The early eruptions were explosive, depositing many cycles of graded pyroclastics. Mid-stage eruptive activity produced 10-30 cm thick lava flows that mantled the growing cone; examples of such flows now appear as outward dipping layers in the center of the quarry (Fig. 6). More explosive eruptions followed, producing the same upward-grading tephra sequences present in the lower parts of the cone. Subsequent volcanic activity produced fluid lava flows which flowed out from the central vent through numerous lava tubes in the cone's base to the northeast.

Aden Cone

Location and Access

Aden cone is located in the Potrillo volcanic field 26 miles southwest of Las Cruces, New Mexico (NW 4, sec. 9, T. 25S., R. 3W.). This cone is most easily reached from the Corralitos exit (exit #27) of I-10, approximately 12 miles west of Las Cruces. A frontage road leads 11 miles southwest from this exit to Aden Station, an abandoned railroad station. From here a paved road leads west 1½ miles directly to the cone(Fig. 2). This deposit has been quarried intermittently for approximately 40 years.

Physiographic Setting

Aden cone, like Santo Tomas Mountain, is included in the Mesilla Bolson which is part of the Mexican Highlands section of the Basin and Range Province (Hawley, 1969). The cone is on the west side of the Aden graben, a structure bounded by the Robledo Fault to the west and the Fitzgerald Fault to the east (DeHon and Reeves, 1965). The Aden Basalt, in which Aden cone is included, appears to be associated with fissures located along the trace of the Robledo Fault (Callahan, 1973).

Geologic Environment

Aden scoria cone is located in the northwest corner of the Aden Basalt (Fig. 11) as defined by

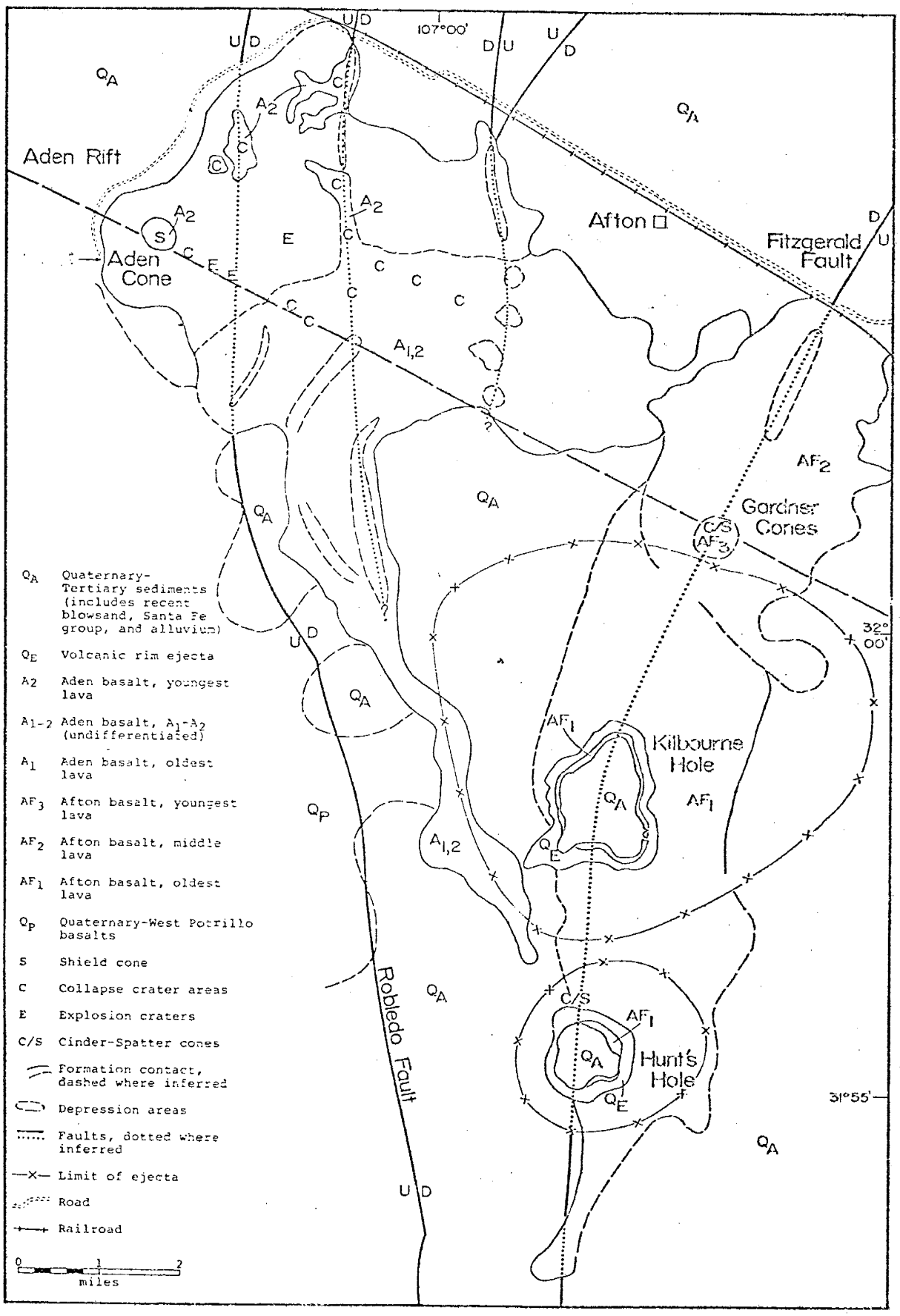

Figure 11: Location map of the Aden Basalt (Hoffer, 1975). Aden cone is shown in the upper left corner.

Kottlowski (1953). Prior to extensive quarrying, the cone rose 88 m above the surface of the Aden Basalt. The base of the cone is elongate in map view, measuring 550 m along the east-west axis and 310 m along the north-south axis. The elongation could be a result of strong wind from the north during the growth of the cone that causes the pyroclastics to build more thickly on the south side of the vent. A late-stage lava flow could have removed material from the north side of the cone.

Pyroclastic Materials

Aden cone is primarily composed of achnelithic, well-sorted tephra. Most of the pyroclastic material (80-90%) is within the lapilli to scoria (1.8-3.8 cm) size range and occurs in beds 0.5 to 8.0 m thick. Larger scoria clasts, from 5-15 cm in diameter, occur as thin beds which separate and define the smaller-grained intervals or sometimes occur as clasts within the finer-grained layers. The beds of larger fragments probably represent eruption pulses somewhat more explosive than those pulses producing smaller clasts. An alternate explanation for the larger-grained beds may be that poorly-defined, graded bedding occurs in Aden cone, similar to the bedding exposed at Santo Tomas Mountain. Blocks and bombs larger than 15 cm make up only a small percentage of all tephra in the cone (Fig. 12).

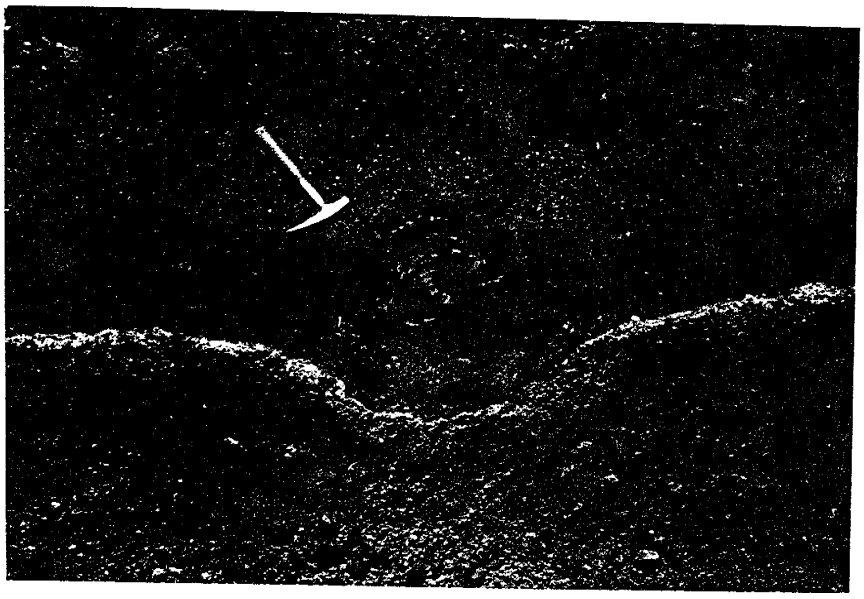

Figure 12: Impact structure in the perimeter of Aden cone. Vertical displacement approximately 20 cm. Hammer at upper left is 33 cm long.

Within the lower 30 m (of 90 m) only blocks occur. These blocks are up to 45 cm across and are widely scattered in the deposit. Blocks and bombs of all types are common in the upper 50 m of the cone. Ropey bombs are the most common form of bomb observed; lesser amounts of ribbon and cowpie bombs occur. Throughout the deposit the blocks and bombs are achnelithic, as are the smaller-sized scoria and lapilli.

The pyroclastic material at Aden cone can be separated into beds on the basis of textural differences, such as the layers of coarse scoria described above. Beds in Aden cone range from 1.5-8.0 m thick in the vent zone, from 0-125 m from the vent; to 0.5-5 m thick in the perimeter zone, at distances greater than 180 m from the vent. In addition to these textural breaks, quiescent periods during the eruptive history of the cone are marked by 3 cm layers of caliche and palagonite-mantled scoria (Fig. 13). The positive identification of caliche was made with a dilute solution of hydrochloric acid in the field as well as later x-ray diffraction tests in the laboratory. Palagonite was identified by visual inspection following the definition of Wentworth and Williams (1932):

> "yellow or orange mineraloid formed by hydration and other alterations of basaltic glass."

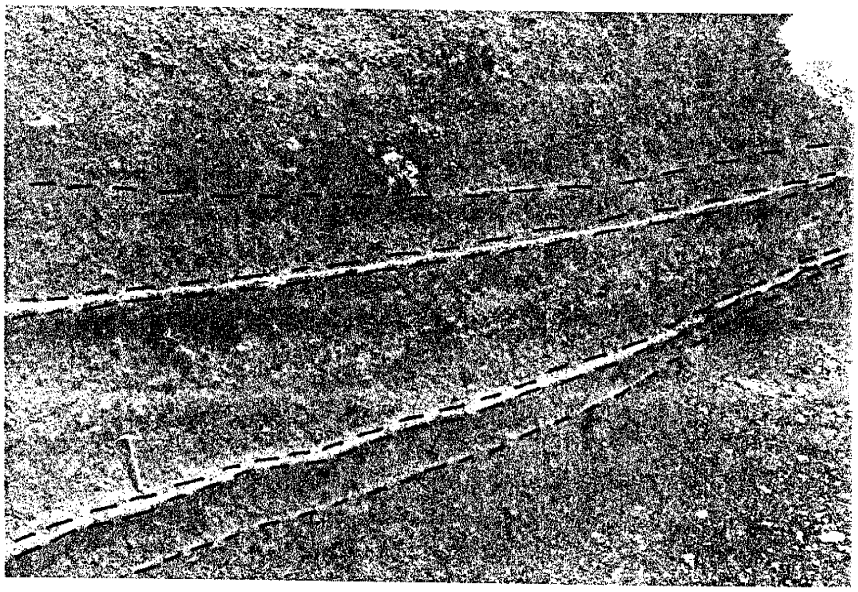

Figure 13: As least four major disconformities marked by thin layers of palagonite and caliche in the perimeter of Aden quarry. Hammer at lower center is 33 cm long.

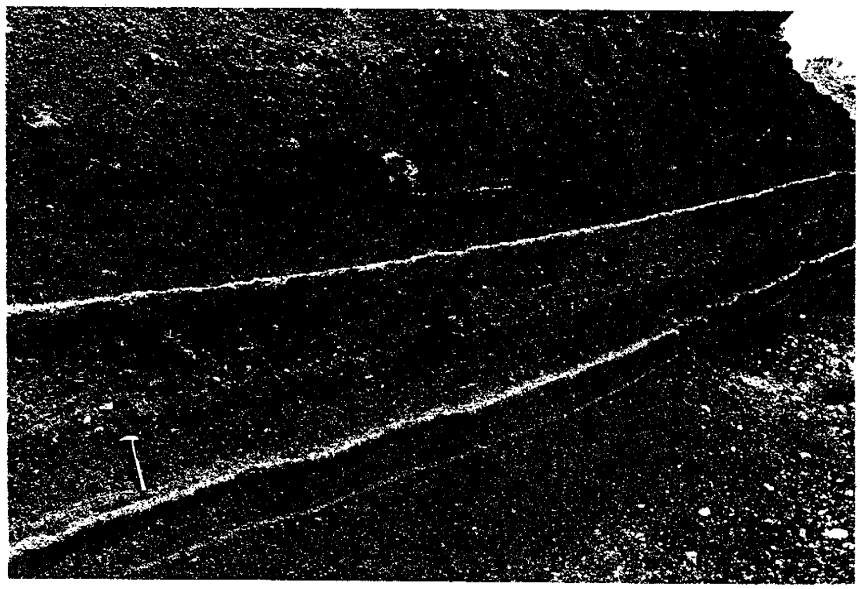

Figure 13: As least four major disconformities marked by thin layers of palagonite and caliche in the perimeter of Aden quarry. Hammer at lower center is 33 cm long.

Eruptive History

A minimum of six eruptive episodes, separated by tens to hundreds of years can be deduced from the field evidence at Aden scoria cone. Strong wind from the north during the eruption could account for the oval shape of Aden cone. Early eruptions were quiet, depositing achnelithic scoria and lapilli with minor amounts of small, angular blocks. Eruption events were separated by periods of quiescence during which caliche and palagonite developed on the exposed slopes by illuviation and alteration of basaltic glass, respectively (Fig. 13). A mimimum of 75 years of inactivity is necessary to develop caliche layers 3 cm thick (Goudie, 1973). Since four of these layers are observed in perimeter cuts of Aden cone, it can be assumed that the cycle of erosion and deposition was repeated a minimum of four times during the eruptive history of the cone. During one of these quiescent periods, it appears that a crater lake developed. A 4.5 m wedge of finely-laminated, buff sand present in the central-east face of the quarry wall marks the position of the crater lake (Fig. 14).

Later eruptions at Aden cone were probably more explosive than the early activity, producing both the scoria found in the outer portions of the cone as well as a wide variety of bombs and blocks. It is common

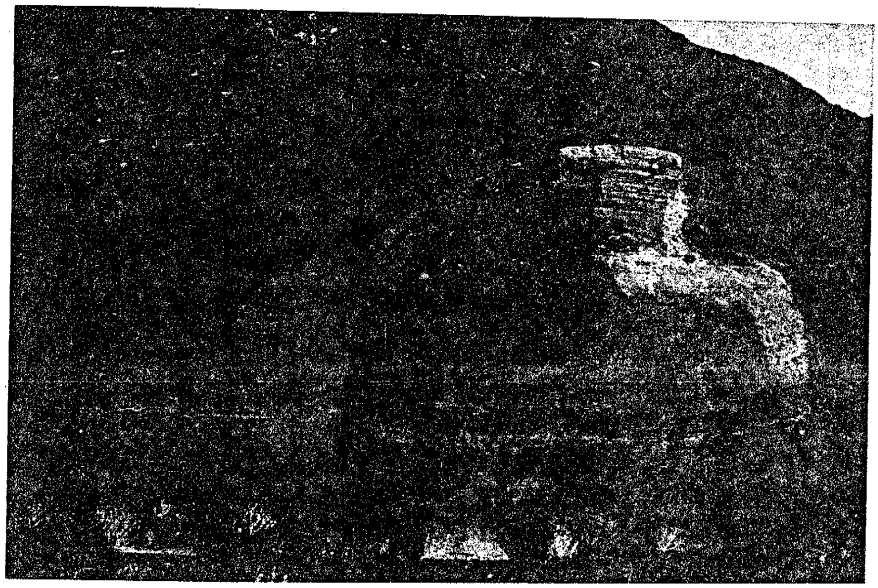

Figure 14: Possible crater-lake sediments consisting of thin-bedded, laminated sand at center right. Wedge of crater-lake sediments is five meters wide.

in scoria cones that bombs and blocks be concentrated in the outer layers of the deposit, perhaps as a result of decreasing gas at the end of an eruption (Macdonald, 1967). Near the end of the eruption of Aden cone, lava flows or explosions could have breached the northern and southwestern rims of the crater. The northern lava flow was of a greater volume or was accompanied by a more violent explosion than the southwestern flow. This can be inferred by the present asymmetrical shape of the cone which suggests that more pyroclastic material was removed from the northern portion of the cone.

Twin Mountain

Location and Access

Twin Mountain is a Holocene scoria cone located approximately 35 miles east of Raton, New Mexico between the small towns of Des Moines and Folsom (SE 4, sec. 19, T. 30N., R. 29E.). Approximately 2 miles southeast of Folsom, a private road (owned by the Colorado and Southern Railroad) leads from New Mexico Highway 72 to the cone (Fig. 15). The deposit has been actively quarried since 1956, providing material for roofing, cinder block, landscaping, and ballast.

Physiographic Setting

Twin Mountain is included within the Raton section of the Southern High Plains region of the Great Plains Province (Fenneman, 1931). The Southern High Plains are characterized by uplifted and canyoned plains with high, lava-capped, dissected mesas (Stobbe, 1949).

Geological Environment

The late Cenozoic volcanic rocks of northeastern New Mexico were erupted onto erosional surfaces cut onto gently warped sedimentary rocks (Stormer, 1972). The volcanic rocks in this area have been divided by Stormer into five distinct groups based on petrography, geomorphology, and age (Fig.15). Twin Mountain is considered part of the Capulin Basalt field which extends from western Union County to eastern Colfax County.

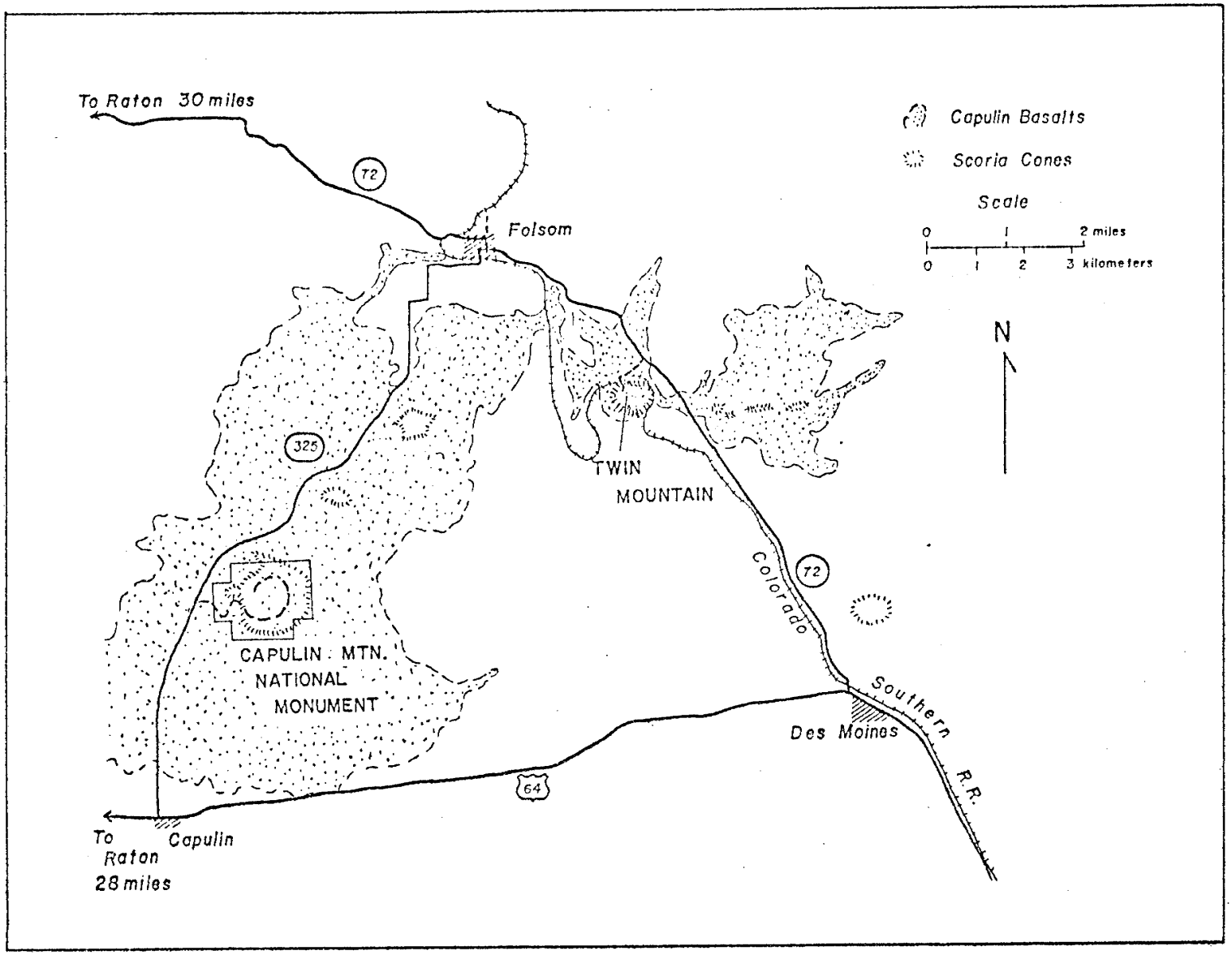

Figure 15: Location map of the Capulin Basalt field showing the location of Twin Mountain scoria cone.

Twin Mountain is an elongated scoria cone 910 m long, 500 m wide, and 80 m high. A trough along the major axis (N 70° E) divides the deposit into two elongate hills. The trough is probably the remains of a cleft-type crater (Fig. 16) formed during the fissure eruption that produced the scoria deposit.

Pyroclastic Material

Most of the tephra at Twin Mountain is lapilli to scoria in size (2-100 mm). Large bombs and blocks up to 60 cm in length are locally abdundant but are not common overall. Bombs 5-15 cm long occur at 2 m horizontal intervals in the lower parts of the deposit. Approximately 80% of the lapilli- to scoria-size clasts are fracture-bound clasts; the remainder are achneliths and spatter.

The distribution of pyroclastic materials and lava flows at Twin Mountain is largely controlled by the nature of the fissure vent. Eruptions probably occurred simultaneously along the length of the vent. Small lava flows, continuous for several hundred feet along the fissure, support this hypothesis. Red agglutinate and red scoria constitute approximately 40% of this deposit, while most of the small-vent cones in the state contain 25% of less of these materials. The red color is due to more intense oxidation and welding of the scoria at Twin Mountain than are seen in other scoria

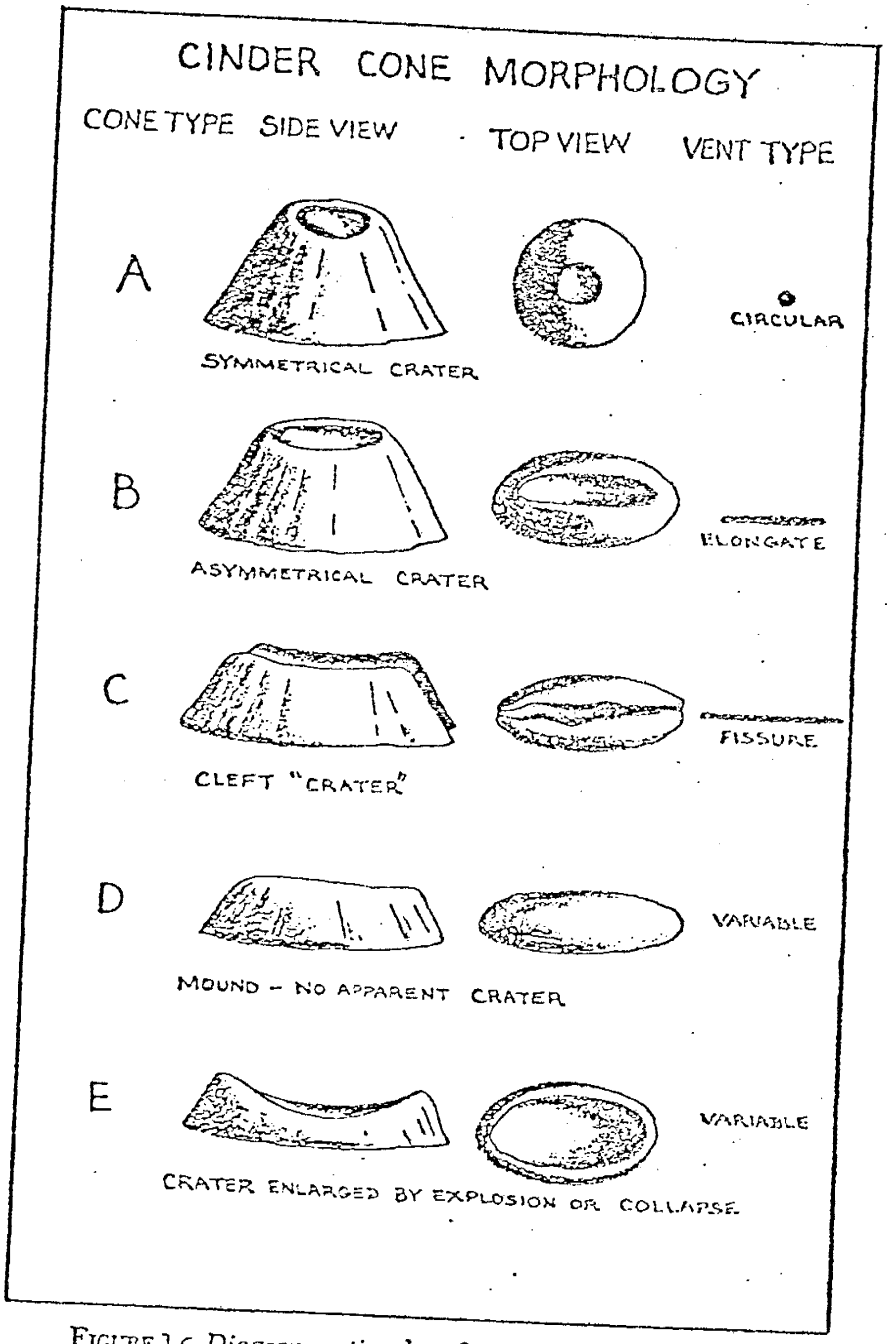

FIGURE 16 *Diagrammatic classification of cinder cones.*
(Breed, 1964)

cones in New Mexico. One explanation for the greater amount of oxidation here, as compared with other cones, is that the fissure vent is larger allowing increased heating of the tephra surrounding the vent (see pages on iron oxidation).

All the pyroclastic material at Twin Mountain is well-stratified. There are few changes in texture of vesicularity of the material with increasing distance from the vent. The main changes are in the color and size of the tephra, and in a sharp decrease in frequency of lava flows away from the vent zone.

The changes in color and size are transitional, but the deposit can be divided into three roughly concentric zones surrounding the vent. For the purpose of discussion, these zones will be called the vent zone, intermediate zone, and the perimeter zone, respectively, based on the relative distance of the zones from the vent and the appearance of the material in each area.

The vent zone (0-125 m from the vent) is made up of 1-3 m layers of dark reddish-brown agglutinate. Thin layers (0.4-1.8 m) of medium-grey, autobrecciated basalt are interbedded with the agglutinate. The agglutinate begins to interfinger with loose, dark red-brown scoria 75-100 m from the vent: and grades completely into loose tephra at 125 m away from the

vent. The basalt flows pinch out completely about 100 m from the vent.

Scoria is the dominant material in the intermediate zone, occuring at distances greater than 125 m from the vent. The scoria in this zone systematically changes color and decreases in size as the distance from the vent increases. The scoria nearest the vent (at 125 m) is dark reddish-brown (5YR 3/2), as is the tephra in the vent zone. At 135 m from the vent the scoria is dark reddish-grey (5YR 4/2) and slightly better sorted than the ventward material. The gradual color change continues to 165 m from the vent where the scoria is dark grey (10YR 4/1) and has green iridescent surface coatings. Bombs in this interval are dark grey also, but have blue rather than green iridescent surface coatings. At 185 m from the vent all material is very dark grey (10YR 4/1) with blue iridescent surfaces.

Tephra greater than 200 m from the vent has been assigned to the perimeter zone. Scoria in this region is consistently very dark grey (10YR 3/1) with no surface iridescence.

This sequence of color variation is regular and can be recognized in all of the cones examined by the writer in New Mexico. This color variation appears to be related to varying degrees of oxidation of the iron

minerals in the scoria and will be discussed further in later sections.

Eruptive History

Twin Mountain was probably built by a short-lived, violent eruption. There are no erosional surfaces to suggest long breaks in the depositional history of the cone. The predominance of fracture-bound clasts suggests a violent eruption (McBirney and Murase, 1970).

The eruption began with the ejection of fracture-bound clasts of scoria and lapilli along the length of the fissure. The tephra closest to the fissure was welded to agglutinate by the intense heat of the eruption. This agglutinate stabilized the crater rim and provided a surface on which alternating lava flows and achnelithic scoria layers were deposited. The presence of both lava flows and abundant achnelithic scoria suggest that the lava was alternately gas-rich and gas-poor during this stage of the eruption. Large amounts of well-bedded, fracture-bound scoria were then deposited stratigraphically above the agglutinate, suggesting that the lava was relatively more gaseous than before. During the final stages of pyroclastic deposition, a large number of blocks and bombs were erupted. These are now exposed at the surface of the unquarried south hill. Later lava flows breached the east and west sides of the cone, after which the eruption ceased.

Blackbird Hill

Location and Access

Blackbird Hill scoria cone is on the Isleta Indian Reservation in Bernalillo County, New Mexico (NE 4, sec. 18, T. 8N., R. 1W.). The cone is reached by way of the Isleta Pueblo exit of I-25 south of Albuquerque, New Mexico. From the exit, drive 10 miles west on unpaved, private road directly to the cone (Fig. 17).

Physiographic Setting

Blackbird Hill is located in the Albuquerque Basin of the Rio Grande depression (Bryan, 1938). This cone is included in a basalt field that rests on the Llano de Albuquerque geomorphic surface (Bachman and Menhart, 1978).

Geological Environment

Blackbird Hill is the northern most of 23 pyroclastic cones, which together with extensive associated basalt flows, are known as the Cat Hills volcanoes (Fig. 17). This vent and others in the Cat Hills are located along a series of north-south trending fissures which roughly parallel the axis of the Albuquerque Basin (Kelley, 1977). Alkali basalt flows beneath the cones flowed from these fissures; later activity along unplugged segments of the fissures produced scoria and spatter cones (Kelley and Kudo, 1978). The basalts surrounding Blackbird Hill are undated; however, similar basalts at Cerros

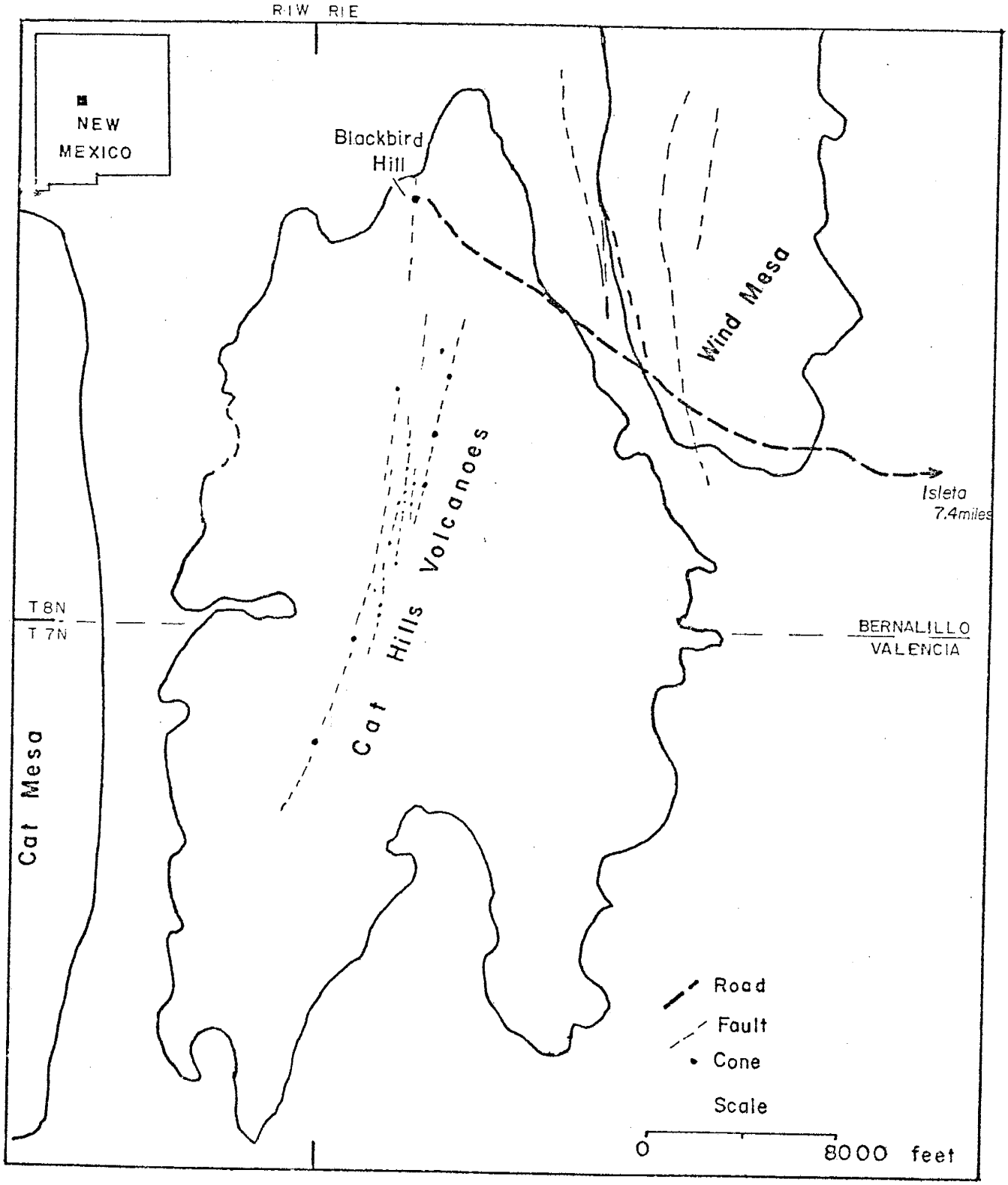

Figure 17: Index map of the Cat Hill volcanoes from Kelley and Kudo, 1978.

Los Lunas on the Llano de Albuquerque surface are dated at 1.01 $\pm$ 0.1 m.y. (Bachman and Menhart, 1978).

The study cone is nearly circular, having a basal diameter of 280 m and is 30 m high. A ring was quarried from the deposit that roughly circumscribes the vent. This cut exposes a wide range of pyroclasitc materials, lava flows, and well illustrates the systematic color variation observed in varying degrees in other scoria cones in New Mexico.

Pyroclastic Materials

Blackbird Hill is composed dominantly of dark grey to very dark-grey, loose scoria. Secondary amounts of loose dark red-brown scoria, agglutinated weak red scoria, and thin lava flows are concentrated in the vent zone of the cone.

Blackbird Hill, like Twin Mountain, can be divided into three zones on the basis of color and distance from the vent. The material in the vent zone (0-40 m) is made up of very poorly-sorted, loose and agglutinated tephra, and outward-dipping lava flows. The tephra is strongly oxidized to a weak red (2.5YR 4/2) color and appears to be most oxidized where the scoria is in contact with lava flows. This suggests that the heat and volatiles, released as the flows cooled, oxidized the tephra. The proportion of aggultinate decreases away from the vent, and is absent at distances

greater than 25 m from the vent. Bombs and blocks present in the vent zone are irregular in shape and range from 5 to 30 cm in size.

The intermediate zone of Blackbird Hill (40-100 m from the vent) is characterized by dark grey, fracture-bound, scoria fragments. The tephra has green iridescent, surface coatings 40-60 m from the vent and blue iridescent coatings 60-80 m from the vent. At distances greater than 80 m, surface iridescence becomes less apparent, and is completely absent at distances greater than 100 m from the vent.

The scoria in the intermediate zone is well-stratified in beds 3-5 m thick. The grain size in each layer remains fairly constant throughout the interval. Few bombs are observed in the intermediate zone, those present are small (less than 10 cm) and are ragged in appearance.

The perimeter zone (greater than 100 m from the vent) is composed of consistently, very dark-grey scoria and minor amounts of small bombs. The pyroclastics are well sorted and bedded in layers 1-3 m thick. A thick (0.5 m) caliche caps the scoria in this zone.

Eruptive History

Blackbird Hill was probably built as a result of a series of closely spaced eruptive pulses. No feature indicative of breaks in the eruptive history of the

cone are observed. The eruption was probably violent, as suggested by the predominance of small, fracture-bound clasts.

GRAIN SIZE CHARACTERISTICS

Samples from various portions of each cone were collected and sieved to observe grain size variations of the scoria in the study cones. Each sample was chosen, at intervals away from the vent, to be within apparent single sedimentation units of limited thickness. Bombs and flows were excluded from sample populations. The sedimentation units were expected to contain a population of fragments erupted by a single eruptive pulse, with only minor amounts of tephra introduced during subsequent eruptions by avalanching and sliding from overlying beds. Sample locations for each study cone are shown in Figure 18 a-d.

The sieve set was chosen to cover a span from -4Ø to 4Ø (from 16 to 1/16 mm) at one Ø intervals (Krumbein, 1936). The sieving was done by hand as suggested by Walker (1971) to minimize abrasion. Raw data was converted to percentage and cumulative percentage figures and was used to construct histograms and cumulative curves for representative samples (Appendix 2).

Parameters used to quantify the size distribution data follow Walker and Croasdale (1971) and Inman (1952).

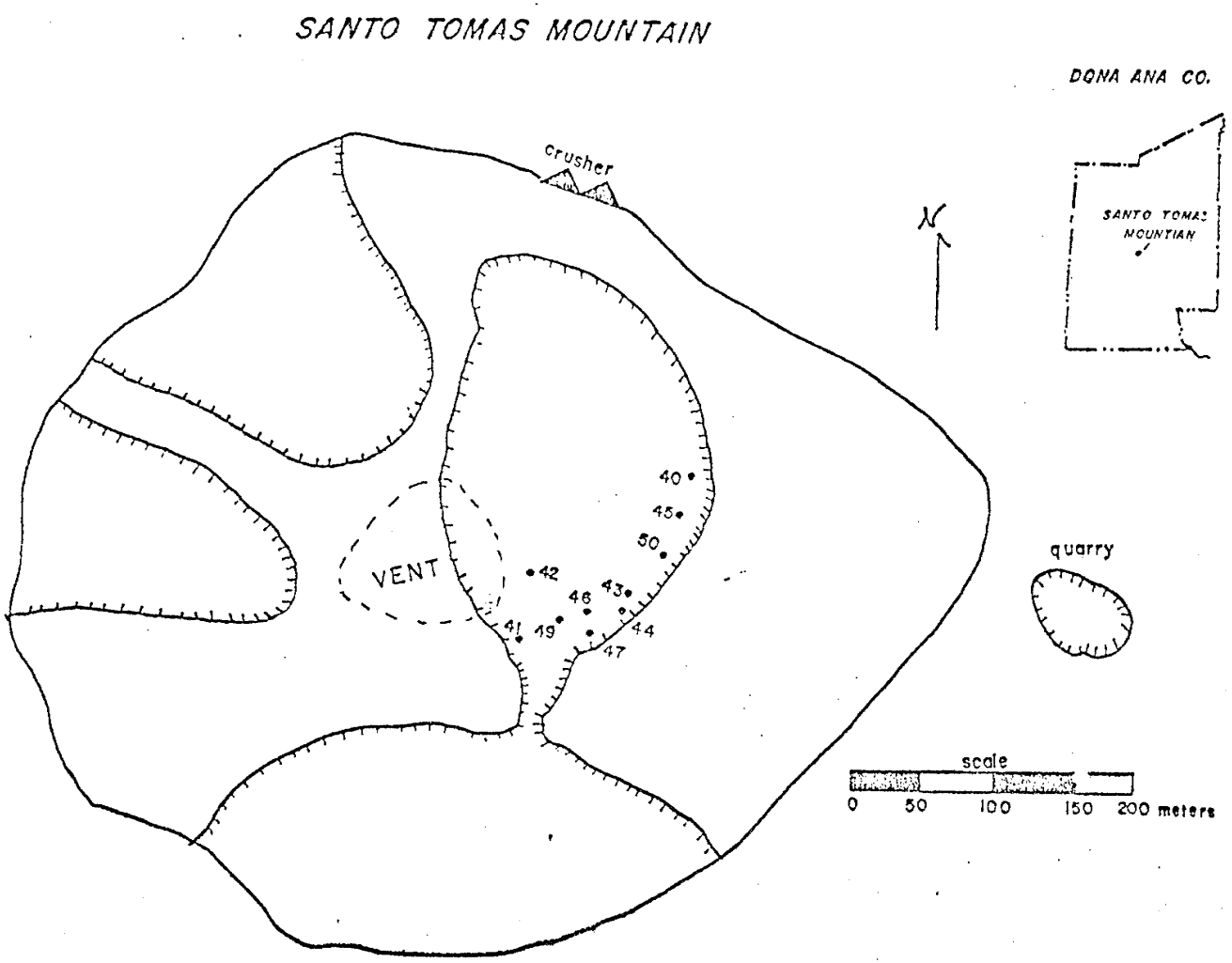

Figure 18 a: Location of sampling stations for the study cones. Approximate boundary between the vent zone and intermediate zone is shown.

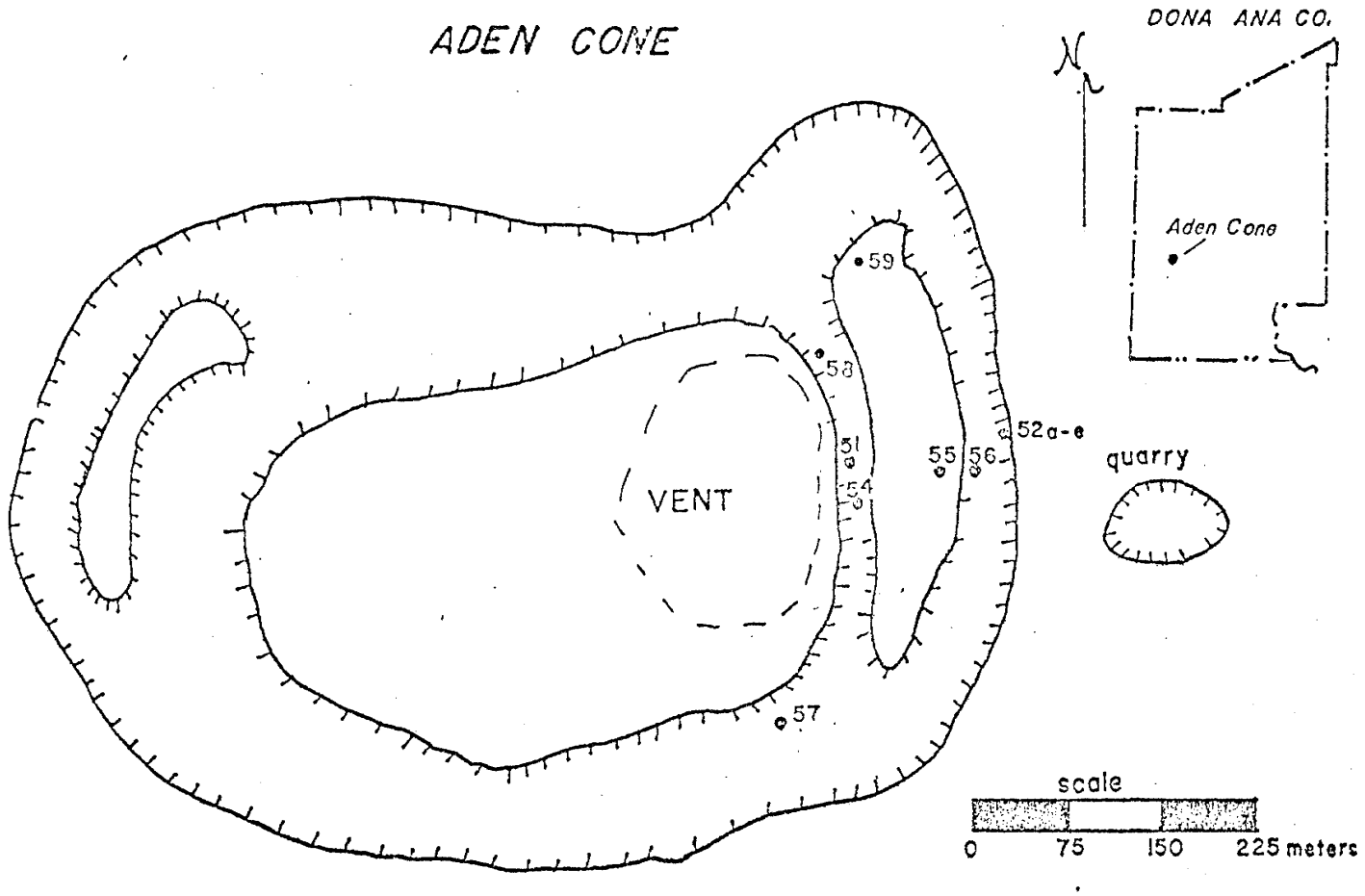
ADEN CONE
DONA ANA CO.
N
Aden Cone
59
58
52a-e
51
54
55
56
VENT
quarry
57
scale
0
75
150
225 meters

Figure 18 b

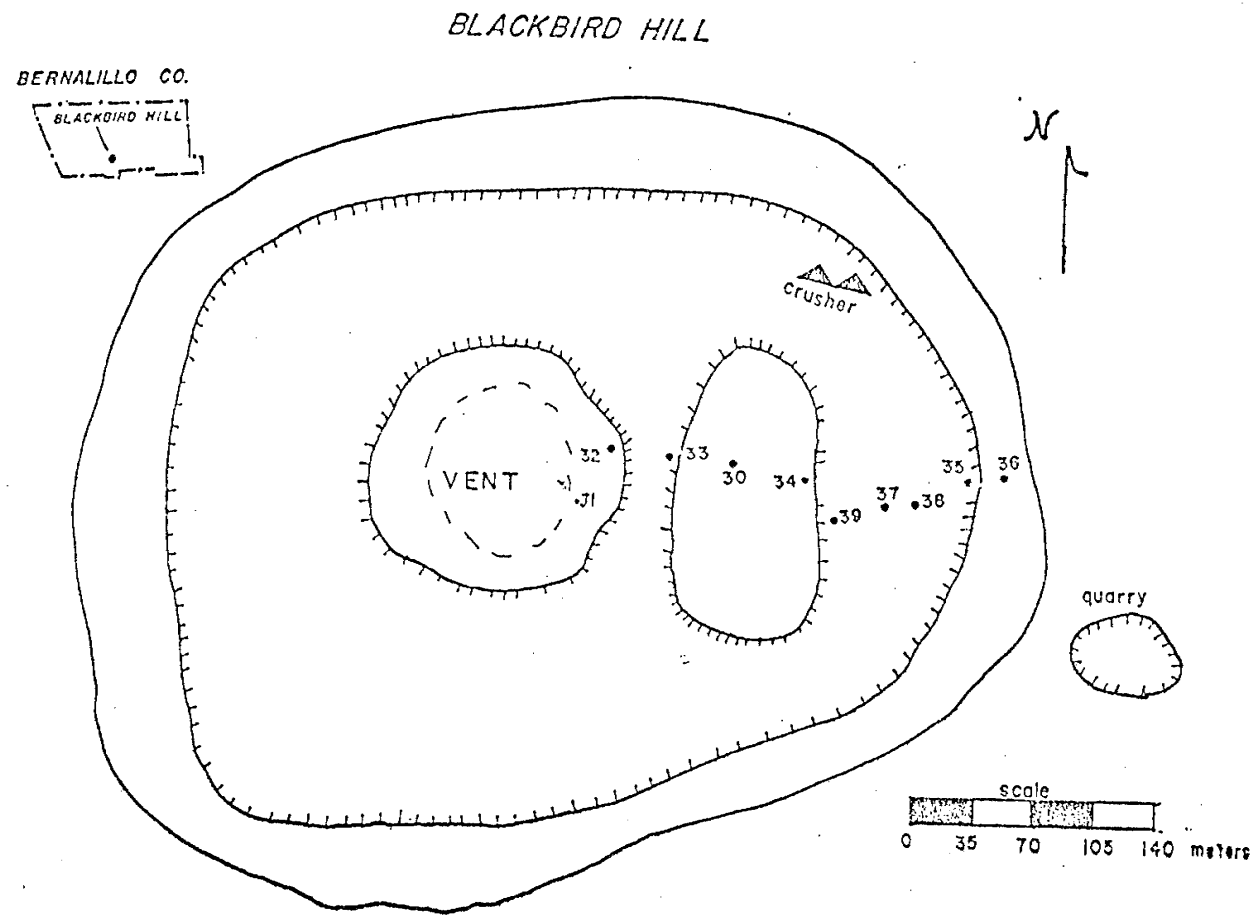
BLACKBIRD HILL
BERNALILLO CO.
BLACKBIRD HILL
N
crusher
VENT
32
31
33
30
34
35
36
37
38
39
quarry
scale
0 35 70 105 140 meters

Figure 18 c

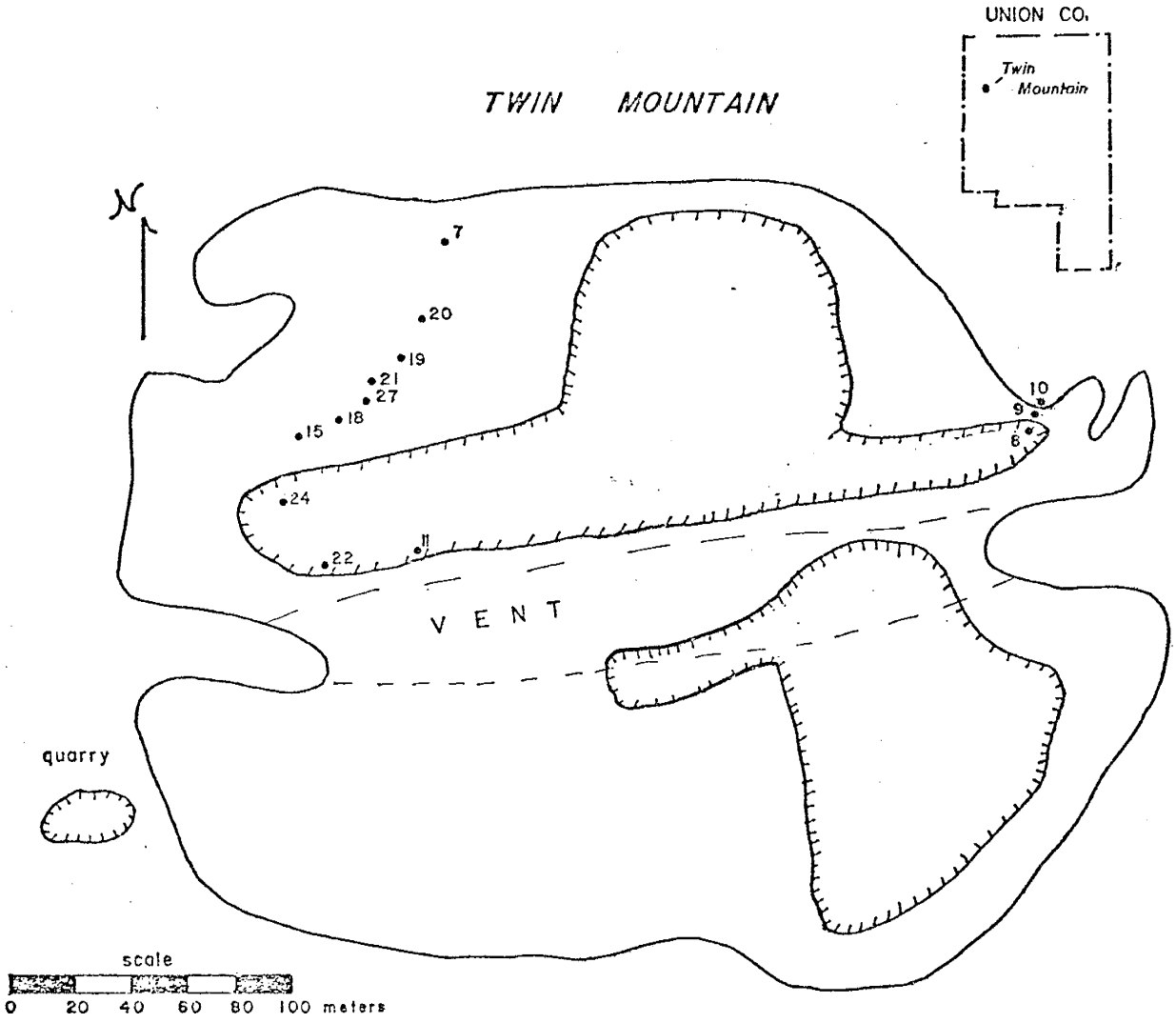
TWIN MOUNTAIN
UNION CO.
Twin Mountain
N
7
20
19
21
27
18
15
24
22
11
10
9
8
VENT
quarry
scale
0 20 40 60 80 100 meters

Figure 18 d

These include median grain size, Mdϕ (the ϕ value which crosses the 50 wt% level), and the degree of sorting, $\sigma\phi$ (½ the distance ϕ between the 16 and 84 wt% levels). These grain size characteristics are shown in Table 2.

The samples ranged from being moderately well-sorted to poorly sorted (Folk, 1965), with over half the samples in the moderately-sorted group ($\sigma\phi$ = 0.99 to 0.25).

Sorting varies consistently within each deposit and within the entire test population. A distance/sorting plot (Fig. 19) shows what was evident in the field; the degree of sorting is directly proportional to distance from the vent. Samples taken within 40 m of each vent are consistently more poorly sorted than anywhere else in a deposit (ϕ = 1.2). Poorer sorting in the vent zone probably results from repeated eruptions mixing and fracturing pyroclastic materials. Larger fragments common in the vent zone tend to trap lapilli and ash which also results in poorer sorting. At distances greater than 80 m from the vent, sample sorting improves and remains at moderate grades (ϕ = 0.9).

Sorting is dependent on fall velocities and varies directly with wind strength (Walker, 1971). Wind influenced the particle distribution of all the study cones, as shown by slight asymmetries in overall cone form. Wind strength was probably exceptionally high

TABLE 2: Grainsize characteristics on samples taken from the study cones. Distance from the vent measured from a fixed point for each cone. Horizontal lines separate vent zone, intermediate zone, and perimeter zone.

Sample	Cone	Distance from vent	σØ	MdØ	MdØ (mm)	Zones
22	Twin Mtn.	15 m	1.27	-3.93	15.24	
24		40 m	1.08	-3.43	10.78	
15		60 m	0.92	-2.37	5.17	
27		70 m	0.72	-2.37	5.00	Vent
21		80 m	1.10	-2.51	5.70	
19		90 m	0.91	-2.21	4.63	
20		105 m	0.95	-2.21	5.70	
07		140 m	0.48	-2.59	6.02	Intermediate
31	Blackbird	12 m	1.52	-2.80	6.96	
32	Hill	25 m	1.39	-2.56	5.90	Vent
30		60 m	1.19	-2.13	4.38	
34		90 m	1.02	-2.42	5.35	Intermediate
39		100 m	0.96	-2.39	5.24	
37		115 m	0.88	-2.26	4.79	Perimeter
38		125 m	0.74	-2.42	6.63	
41	Santo	10 m	1.30	-3.81	14.02	Vent
47	Tomas	60 m	1.26	-3.77	13.64	
44	Mtn.	90 m	0.82	-3.47	11.08	Intermediate
43		100 m	0.71	-3.42	10.70	
50		120 m	1.13	-3.47	11.08	
45		135 m	1.03	-3.63	12.03	Perimeter
40		150 m	0.69	-3.38	10.41	
51	Aden	10 m	1.40	-3.30	9.85	
54	Cone	50 m	0.84	-3.20	9.19	Vent
55		90 m	0.85	-3.25	9.15	
52B		150 m	0.80	-3.00	8.00	
52D		150 m	0.81	-3.03	8.17	Intermediate
52E		150 m	0.84	-2.71	6.54	

$Md\phi = 8.40 \pm 3.07$ mm

$\sigma\phi = 0.99 \pm 0.25$

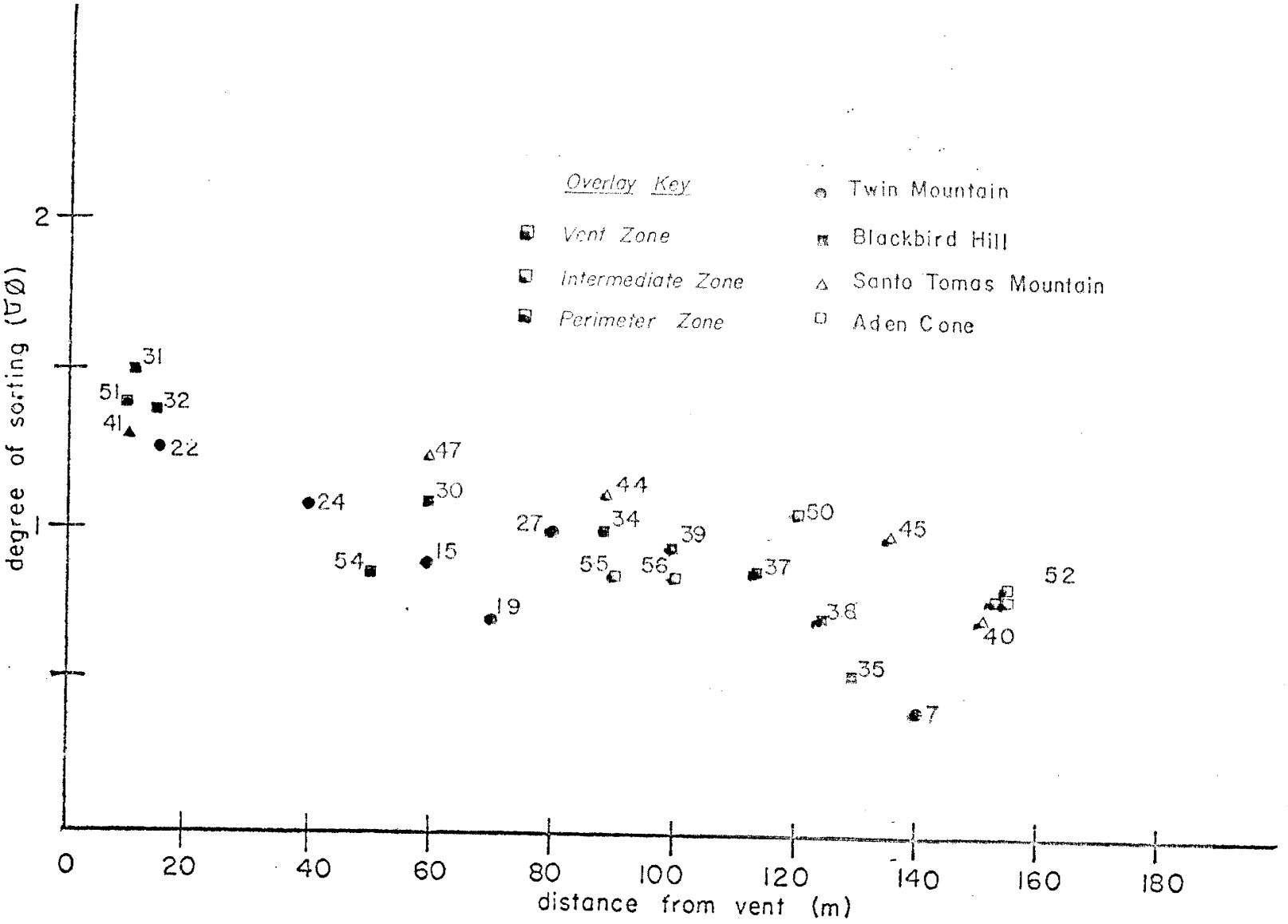

Figure 19: Degree of sorting of the samples plotted against the distance of the sample from the vent.

during the eruption of Aden cone. This is supported by consistently good sorting evident at distances greater than 40 m from the vent. If the wind were strong, all materials could be equally sorted according to their respective fall velocities (Walker, 1971).

The median grain size varies systematically within a given cone but little from cone to cone (Fig. 20). The largest and most variable fragments (8-16 mm) fall within 60 m of the vent in each study cone. At distances greater than 60 m, the median grain size is between 5 and 11 mm for all deposits. Within each cone, the median grain size is probably varies relative to the geometry of the cone especially for the intermediate and perimeter zones. The small differences in average grain size among cones can probably be explained by differences in the viscosity, water vapor, and composition of the respective magmas (Macdonald, 1971). The character of the magma could ultimately control the strength of the eruption, the density of individual clasts, and the fall velocities of individual clasts. Local ground water conditions could also influence the eruption products.

The median grain size varies inversely with the degree of sorting in each study cone but does not vary consistently throughout the entire sample population (Fig. 21). The plot shows that the median grain size

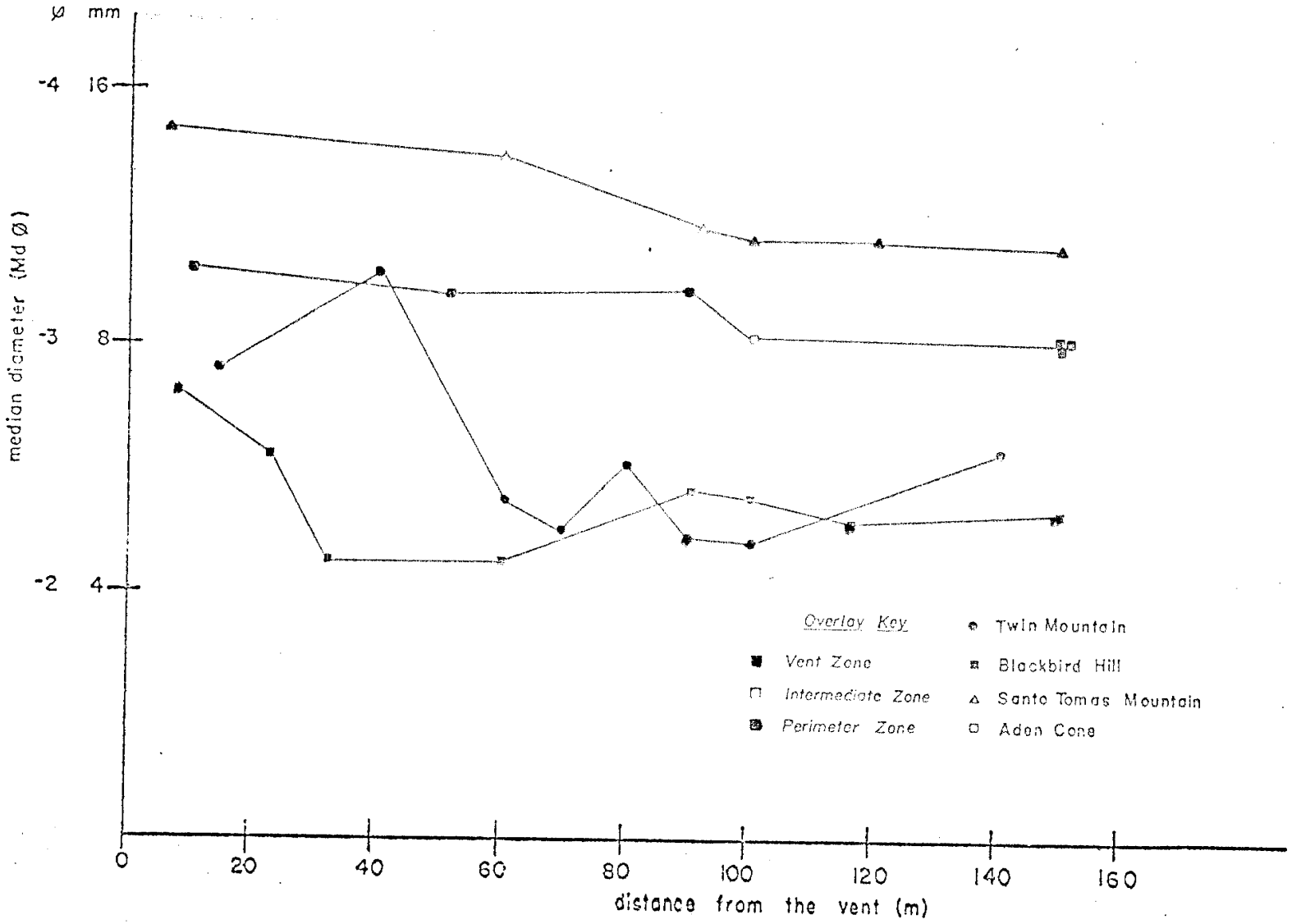

Figure 20: Median diameter of a sample plotted against the sample's distance from the vent.

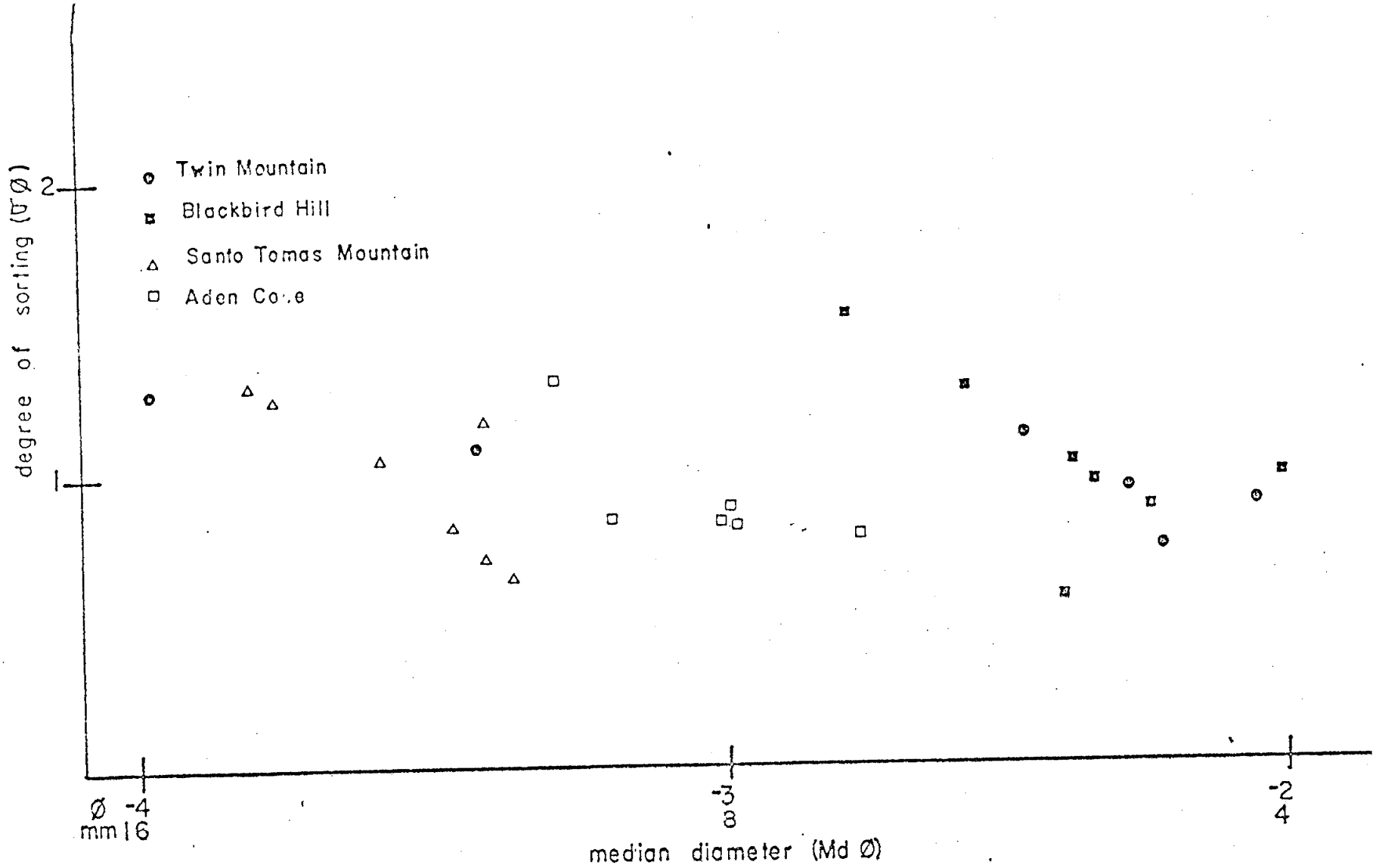

Figure 21: Degree of sorting for each sample plotted against the median grain-size of each sample.

range varies from cone to cone. It therefore appears that median grain size is subordinate to distance from the vent in determining the average degree of sorting in a given cone.

SCORIA COLOR VARIATIONS

The three-zoned color pattern found in all the opened scoria cones in New Mexico as part of this study is not discussed in the literature. Two-color variation (red scoria and black scoria) has been noted before but was seldom examined in any detail.

Parker (1963) suggested that red scoria exposed at Amboy Crater in California was produced as a result of eruption during a rainy period. Walker and Croasdale (1971) noted a tendency for scoria cones in Hawaii to show some reddening around the vent which they attributed to oxidation by steam during the course of the eruption. The upper surface layer of many scoria cones in New Mexico are reddened for depths of a few centimeters, suggesting a weathering origin for the coloration.

Some or all of the above factors probably do contribute to the color patterns present in scoria cones. However, the common occurrence of the pattern suggests that the causative factor of the coloration pattern was common to all cones examined, regardless of magma, geographic location, weather conditions during the eruption, or strength of the eruption. It was noted that the same color variation is present on a smaller

scale adjacent to small lava flows within the cones. Heat associated with the eruption was hypothesized to largely control the color variation both on a local and "total cone" scale. Heating tests in the laboratory were conducted to simulate eruption conditions and test this hypothesis.

Oxidation State of Iron

Chemical tests were conducted to learn if the observed color variations in a given scoria cone reflect variation in the oxidation state of iron in the tephra. The population of samples chosen from each cone was selected to give maximum possible variation in color and distance. Sample locations for each cone are shown in Figure 18 a-d.

The samples were crushed and prepared for analysis using standard preparation methods for analysis by atomic absorption spectrometry used at New Mexico Bureau of Mines and Mineral Resources (Brandvold, 1974). The amount of ferrous iron in the samples was determined by titrating the samples with a 0.05 N solution of potassium dicromate. Total iron was determined by atomic absorption spectrometry using a Perkin-Elmer Model 303.

The raw chemical data was converted to a ratio of ferrous iron to total iron in each sample (Table 3), and was plotted against the distance from the vent for each sample (Appendix 4).

The amount of ferrous iron present in each sample varies directly with the distance from the vent. The amount of ferrous iron levels out to 20 - 30% of total iron approximately 75-100 m from the vent

The chemical data correlates closely to the observed, systematic color variation. The tephra within 50 m of

TABLE 3

Sample	Distance from vent	Fe^{+2}	Fe_t	Fe^{+2}/Fe_t	Munsell	Color
22	015	0.54	8.04	0.06	5YR 4/2	dk red grey
24	040	2.24	8.09	0.28	5YR 3/3	dk red brown
18	050	2.79	7.90	0.35	10YR 3/1	dk red grey
27	070	3.83	7.67	0.50	7.5YR N3/	v dk grey
21	080	4.80	9.05	0.53	5YR N3/	v dk grey
19	090	5.37	8.95	0.60	5YR N3/	v dk grey
20	105	5.36	7.90	0.68	7.5YR N4/	v dk grey
07	140	5.77	8.02	0.72	10YR 3/1	v dk grey
31	015	0.44	8.80	0.05	2.5YR 4/2	wk red
32	025	1.02	8.50	0.12	5YR 3/3	dk red brown
33	035	3.78	8.22	0.46	5R 3/1	dk red grey
34	085	6.61	8.50	0.78	5YR N3/	v dk grey
35	130	7.39	8.40	0.88	5YR N3/	v dk grey
36	150	7.39	8.30	0.89	10YR 3/1	v dk grey
41	010	0.59	8.40	0.07	2.5YR 4/2	wk red
49	020	1.38	7.83	0.18	5YR 3/3	dk red brown
42	020	1.55	8.19	0.19	5YR 3/3	dk red brown
46	030	1.50	7.60	0.20	5R 3/1	dk red grey
47	060	2.40	7.95	0.30	7.5YR N3/	v dk grey
44	090	3.77	7.86	0.48	7.5YR N3/	v dk grey
43	100	3.77	7.75	0.49	2.5YR 3/1	v dk grey
50	120	4.95	7.80	0.64	7.5YR N3/	v dk grey
51	010	0.31	8.03	0.04	2.5YR 4/2	wk red
55	090	1.76	8.74	0.20	7.5YR N3/	v dk grey
56	100	1.97	8.72	0.23	7.5YR N3/	v dk grey
52A	150	5.66	8.53	0.66	2.5YR N3/	v dk grey
52B	150	6.23	9.14	0.68	2.5YR N3/	v dk grey
52C	150	6.55	9.15	0.72	2.5YR N3/	v dk grey
52D	150	6.59	7.48	0.88	5Y 3/1	v dk grey
52E	150	5.98	9.28	0.64	5Y2.5/1	black
57	180	6.60	8.80	0.75	5Y 3/1	v dk grey

each vent is weak red to dark red-brown in color and has ferrous to total iron ration of 0.02 - 0.30. The color (Appendix 1) of the material becomes less red with increasing distance from the vent.

In the intermediate zone from the vent, the scoria has a ferrous to total iron ratio of 0.30-0.60 and is dark to very dark-grey with green to blue iridescent coatings on surfaces of the fragments. The color changes from dark grey to very dark-grey and the iridescence from green to blue moving away from the vent. Green iridescence is not always widespread enough to recognize as a zonation. Often very dark-grey scoria with primarily blue iridescence will be mixed with lesser amounts of scoria with green iridescence. Conversely, at Twin Mountain bombs with blue surface coatings are found in a zone where green iridescence is common. This suggests that the partial oxidation phenomenon is highly dependant on variations in the physical properties of the tephra including size, surface area, and porosity as well as the properties of the lavas including composition and water content.

The scoria in the perimeter zone of each cone tends to be consistently very dark-grey in color with no surface iridescence. The ferrous to total iron ratios are between 0.60 and 0.90. Unlike the vent or intermediate distance zones, there are no gradational changes in

color. Likely this very dark-grey color (usually 10YR N3/), represents the initial color of the scoria as it is deposited.

Samples were collected from Aden cone to investigate possible vertical variation in ferrous iron to total iron. Samples 52 A-E represent a vertical succession of scoria 150 m from the vent exposed in a northern wall of the cone (Fig. 13). The samples appear identical in color (2.5YR N3/) and average grain size (-3.0Ø), and still show variation in the oxidation state of iron. A gradual increase in the proportion of ferrous iron occurs vertically in the section. Other vertical sections closer to the vent at Aden show color changes from dark red-brown to dark grey with increasing vertical distance. Vertical color variation is more difficult to categorize than the three-zoned, horizontal variation. Like the horizontal change, vertical color variation is gradational and appears unrelated to depositional events, crossing layer boundaries.

Examining the horizontal decrease in oxidation outward and the vertical decrease in oxidation upward, the influence of the vent is evident. The oxidation of the iron minerals in the scoria appears to be a result of the release of heat and/or volatiles at the vent during and shortly after the eruption ceases.

Scoria is an excellent insulating material with a thermal conductivity of 3.5k (Schmidt, 1956). This property probably enhances the oxidation pattern found in scoria cones. As each layer of material is deposited, the hot conduit is further insulated from the outer portions of the cone, thus producing the observed color pattern.

Heating Tests

Samples from the study cones were heated to induce oxidation of the iron minerals in the scoria. An attempt was made to reproduce the colors of the tephra seen in the field, in the laboratory. The samples were chosen such that each individual clast in the sample was of the same color. All parts of the cones were sampled to learn if oxidation of iron could be induced on both virtually unoxidized samples as well as partially oxidized samples. Both crushed and fragmental samples were put into small crucibles and heated at various temperatures for various amounts of time in a preheated, Blue M muffle furnace. The color of the samples was visually matched to the Munsell Soil Color Chart (1973) both prior to heating and after the samples were cooled completely (Appendix 4).

Various temperatures and periods of exposure were examined in the initial phases of the experiment to test the validity of using heat to induce oxidation of pyroclastic materials. Finally, two temperatures were selected to test a large number of samples, 400^{o}C and 700^{o}C. These temperatures were chosen because these are within the range of temperatures expected within an erupting and cooling scoria cone. Furthermore, it was found that scoria heated to temperatures less than 400^{o}C showed no detectable color change after several

days exposure, while temperatures greater than 700°C oxidized the iron in the scoria too rapidly to accurately record the oxidation colors.

Samples were exposed to 400°C temperatures for periods of 12, 24, 42, and 84 hours. As would be expected, the crushed samples were oxidized more rapidly than the fragmental samples. The samples changed color very slowly at this temperature. Often it was possible to discern a visual change by comparing the heated sample with an unheated sample, but the difference would not be large enough to merit a different Munsell notation. Some samples did not change notably throughout the test period. Other samples changed only in Munsell designation, for example, from 2.5Y N3/ to 10YR 3/1, while remaining very dark grey in color name. In general, when color change did occur, the hue designation become consistantly more red, the chroma approached moderate saturation, and the value increases (Fig. 22). These changes collectively indicate a lighter, more saturated color.

Samples were exposed to 700°C temperature for periods of 1, 2, 3, 4, and 8 hours. An orderly progression of oxidation steps could be observed with time. In most cases, recordable change was visible after one hour of exposure time. The surface iridescence noted in the intermediate zones of all study cones was reproduced in most samples after 3 hours of heating. After

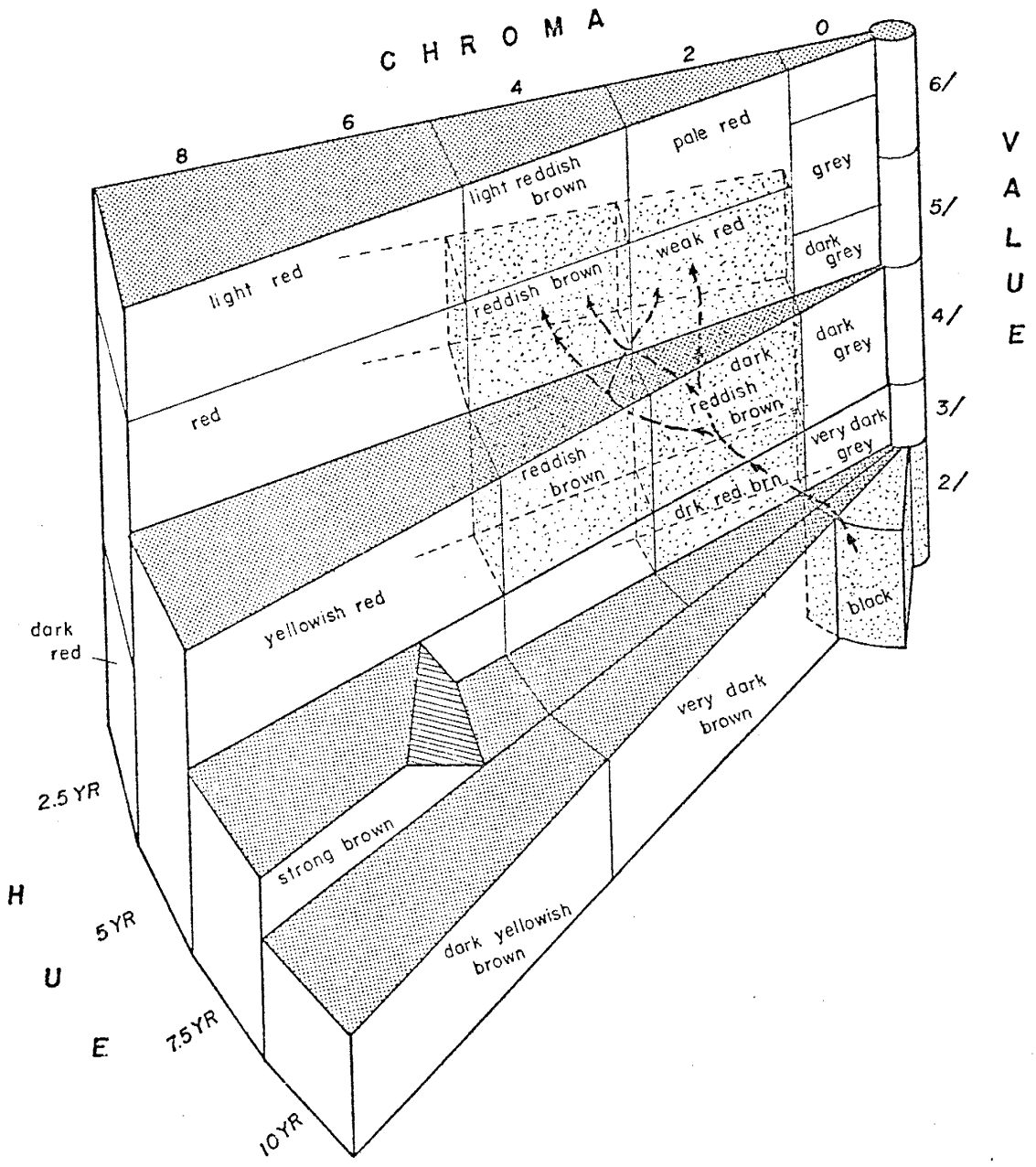

Figure 22: Typical color variation observed when scoria is heated and oxidized.

surface iridescence was produced, dark red-brown 'flakes' were visible on the surfaces of the iridescent fragments. With more heating, more 'flakes' appeared, eventually coalescing to form a dark red brown crust on the outer surfaces of the fragments. Yellow brown crusts appeared on some of the samples after they were mostly dark red-brown in color. These crusts possibly are palagonite, formed by the devitrification of basaltic glass. Alternately, these crusts could represent an iron alteration mineral such as goethite. Oxidation is apparently maximized when the samples are weak red in color as no further color change is observed after the appearance of this color. Maximum oxidation of iron at this point is supported by weak red samples taken from the study cones; in which 93-97% of the iron in the samples occurred in the oxidized state.

It is difficult and perhaps unwise to compare stringently actual temperature conditions of an erupting scoria cone with the experimental heating tests. However, several trends in coloration appear in both situations. The amount of oxidation of iron minerals in the scoria increases with time and temperature of reaction until equilibrium is reached. Color zones in the field and the heating data show the scoria has a color distribution related to temperature zoning around

the cone. Individual fragments of scoria do not oxidize at the same rate, regardless of temperature conditions. Physical properties such as porosity, composition and surface area are probably involved.

ECONOMIC SIGNIFICANCE

Ten scoria cones are currently being mined in New Mexico. The primary use of scoria in the state is the manufacture of lighweight cinder blocks. Smaller amounts of scoria are used as decorative aggregate for roofing materials and for landscaping.

Extraction Methods

Extraction of scoria is a relatively simple surface mining operation. Overburden is stripped from the cone by pushing the surface debris downhill with a bulldozer. The scoria is loosened using a bulldozer blade and a ripper. Blasting is sometimes necessary to free scoria under lava flows within the cone. The useable scoria is extracted with a bulldozer or front-end loader and then moved by conveyor belt or truck to an aggregate processing plant (Fig. 23). The aggregate processing plant crushes, cleans, and screens the scoria. The processed aggregate is then transported by truck or rail to the marketplace.

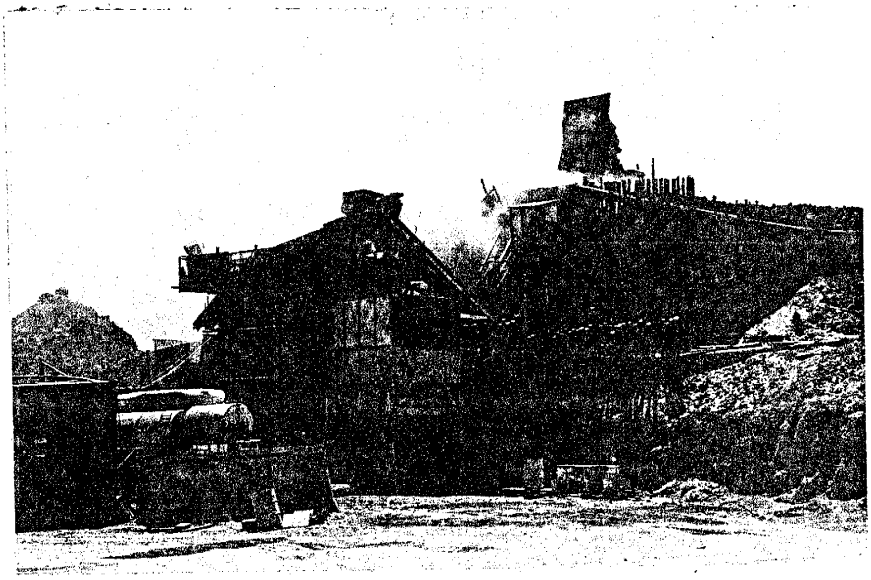

Figure 23: The Aggregate processing plant at Santo Tomas Mountain. Raw aggregate is dumped in the top of the plant and crushed to the desired size. Sized aggregate is held in the lower storage bin awaiting transporation by truck.

Significance of Study to Quarrying Operations

Scoria cones have been successfully quarried for many years without using geology as a tool. However, understanding the predictable spatial relationshps among the different materials in the deposits based on geology could make quarrying operations more efficient.

The potential market of scoria is dependent on both size distribution of the clasts and color of the material. The size of the marketable aggregate is largely controlled by crushing and screening. However, large amounts of waste materials such as ash or lava flow material decrease the value of the product. Early portions of this study have shown that all successful quarrying operations in New Mexico are in cones with aspect ratios (height/basal diameter) of 0.10 to 0.20. Quarrying only cones with aspect ratios within this range would surely lower waste, which would in turn, lower production cost per cubic yard of useable material.

The color of volcanic aggregate is becoming very important, particularly in the growing landscaping and roofing markets. Knowledge of the characteristic color zoning in scoria cones would enable the operator to predict probable locations of the various colors of scoria. Using this type of knowledge, the number of test pits, often dug to determine color and quality, could be reduced.

CONCLUSIONS

In four scoria cones studied in New Mexico - Twin Mountain, Blackbird Hill, Santo Tomas Mountain, and Aden Cone, - characteristic color zoning is observed. This color zoning corresponds to variation in the oxidation state of iron minerals in the tephra. This pattern is roughly vent-centered with dark red-brown material adjacent to the vent, grading to very dark-grey color in the perimeter zone. Iridescent surface coatings on clasts at intermediate distances may reflect partial oxidation of iron. Laboratory tests have shown that heat will induce iron oxidation in scoria, and is likely to be the cause of the coloration pattern observed in scoria cones. Knowledge of the color pattern could be used to quarry scoria deposits more efficiently, enabling the operator to predict the color and quality of material in different portions of a given cone.

Pyroclastic materials in scoria cones in New Mexico are similar in size, shape, sorting, and stratification to those discussed in the literature in Hawaii, Mexico, and Arizona. Pyroclastic fragments present in the study cones are of two textural types: achnelithic and fracture-bound. Achneliths are most abundant in beds

containing ropey bombs suggesting that lower viscosity magma favors the presence of achneliths.

Sorting and stratification show a consistent pattern within a given cone and for all cones studied. The degree of sorting generally increases directly with distance from the vent. Average diameter of the clasts decreases with distance from the vent for each cone but varies from cone to cone. This probably reflects differences in magma composition and viscosity.

REFERENCES CITED

Bachman, G. O. and Menhart, H. H., 1978, New K-Ar dates and the late Pliocene to Holocene geomorphic history of the central Rio Grande region, New Mexico: Geol. Soc. America Bull., v. 89, p. 283-294.

Breed, W. J., 1964, Morphology and lineation of cinder cones in the San Francisco volcanic field: Museum of Northern Arizona Bull., v. 40, p. 65-71.

Bryan, Kirk, 1938, Geology and ground-water conditions of the Rio Grande depression in Colorado and New Mexico: Washington Regional Planning pt. 6, Rio Grande Joint Inv. Upper Rio Grande Basin, Nt. Res. Comm., v. 1, pt. 2, sec. 1, p. 197-225.

Brandvold, L. A., 1974, Atomic absorbtion methods for analysis of some elements in ores and ore concentrates: New Mexico Bureau of Mines and Mineral Resources Circ. 142, 22 p.

Bullard, F. M., 1963, Volcanoes in History, in Theory, in Eruption: Austin: University of Texas Press, p. 11-13.

Callahan, C. J., Jr., 1973, Aden Basalt volcanic depressions, Dona Ana County, New Mexico: unpublished M.S. thesis, Univ. of Texas, El Paso 82 p.

Colton, H. S., 1937, Cinder cones and lava flows: Museum of Northern Arizona Bull. 10, 58 p.

Cotton, C. A., 1944, Volcanoes as Landscape Forms: New York, Hafner Publishing Co., Inc., p. 141-151.

DeHon, R. H., 1965, The Aden crater lava cone: Compass, v. 43, p. 34-40.

_____ and Reeves, C. C., 1965, Geology of the Potrillo maar, New Mexico and Chihuahua, Mexico: Am. Jour. Sci., v. 263, p. 401-409.

Fenneman, N., 1931, Physiography of the Western United States: McGraw-Hill Book Co., New York, 534 p.

Fisher, R. V., 1961, Classification of volcanoclastic sediments and rocks: Geol. Soc. America Bull., v. 72, p. 1409-1414.

Folk, R. L., 1965, Petrology of Sedimentary Rocks: Univ. of Texas, Austin, Hemphills, 169 p.

Francis, P. W. and Thorpe, R. S., 1974, Significance of lithologic and morphologic variations or pyroclastic cones: Geol. Soc. America Bull., v. 85, p. 927-930.

Green, N. L., 1975, The Cinder Cone: a Pleistocene eruptive center, Garibaldi Park, south western British Columbia (abs.): Geol. Soc. America Abstr. with Programs, v. 7, no. 16, p. 767.

Goudie, A. S., 1973, Duricrusts in Tropical and Subtropical Landscapes: Oxford, Claredon Press, 174 p.

Hawley, J. W. and Kottlowski, F. E., 1969, Quaternary geology of the south-central New Mexico border region: in Border Stratigraphy Symposium, New Mexico Bureau of Mines and Mineral Resources Circ. 104, p. 89-115.

Hoffer, J. M., 1975, The Aden-Afton basalt, Potrillo volcanics, south-central New Mexico: Texas Jour. Sci., v. 26, p. 379-390.

_____, 1973, Summary of Cenozoic geology of southern Dona Ana County, New Mexico: El Paso Geol. Soc., 7th Annual Fieldguide, P. 1-15.

_____, 1971, Mineralogy and petrology of the Santo Tomas-Black Mountain basalt field, Potrillo volcanics, south-central New Mexico: Geol. Soc. America Bull., v. 82, p. 603-611.

_____, 1969, Volcanic history of the Black Mountain-Santo Tomas basalts, Potrillo volcanics, Dona Ana County, New Mexico: New Mexico Geol. Soc., Guidbook 20th field conf., p. 108-115.

Inman, D. L., 1952, Measures of describing the size distribution of sediments: Jour. Sed. Pet., v. 22, p. 125-145.

Kelley, V. C., 1977, Geology of Albuquerque Basin, New Mexico: New Mexico Bureau of Mines and Mineral Resources Mem. 33, 58 p.

_____ and Kudo, A. M., 1978, Volcanoes and related basalts of Albuquerque Basin, New Mexico: New Mexico Bureau of Mines and Mineral Resources, in press.

Kottlowski, F. E., 1953, Tertiary-Quaternary sediments of the Rio Grande Valley in southern New Mexico: in Guidebook of Southwestern New Mexico: New Mexico Geol. Soc. 4th field conf., p. 144-148.

Krumbein, W. C., 1936, Application of lograithmic moments to size frequency distribution of sediments: Jour. Sed. Pet., v. 6, p. 35-47.

Macdonald, G. A., 1967, Forms and structures of extrusive basaltic rocks: in Basalts, the Poldervaart Treatise on Rocks of Basaltic Composition, Interscience Publishers, New York 482 p.

McBirney, A. R. and Murase, Thomas, 1970, Factors governing the formation of pyroclastic rocks: Bull. Volc., v. 34, p. 372-384.

Munsell Products, 1973, Munsell Soil Color Charts: Baltimore, Maryland, Munsell Products, unpaged.

Parker, R. B., 1963 Recent volcanism at Amboy Crater, San Bernardino County, California: Calif. Div. Mines and Geology Sp. Rep. 76, 22 p.

Porter, S. C., 1972, Distribution, morphology and size frequency of cinder cones on Mauna Kea volcano, Hawaii: Geol. Soc. America Bull., v 83, p. 3607-3612.

Rittman, A. L., 1962, Volcanoes and Their Activity, translation by E. A. Vincent: Interscience Pub., New York, 300 p.

Schmidt, R. Sommer, 1956, Technology of Pumice, Pumicite and volcanic cinders: California Div. Mines, Bul. 174, San Francisco, 117 p.

Stobbe, H. R., 1949, Petrology of the volcanic rocks of northeastern New Mexico: Geol. Soc. America Bull., v. 60, p. 1041-1095.

Stormer, J. C., Jr., 1972, Ages and nature of volcanic activity on the southern High Plains, New Mexico: Geol. Soc. America Bull., v. 83, p. 2443-2448.

Thorarinsson, S. R., 1954, The tephra fall from Hekla on March 29th, 1947, in The Eruption of Hekla 1947-1948: Soc. Sci. Islandica, Rejkjavic, 68 p.

Tsuya, H. A., 1941, On the form and structure of volcanic bombs, from Volcano Miyakesima: Bull. Earthquake Res. Inst., v. 19, p. 597-611.

Walker, G. P. L., 1971, Grain size characteristics of pyroclastic deposits: Jour. Geology, v. 79, p. 696-714.

Walker, G. P. L. and Croasdale, R., 1971, characteristics of some basaltic pyroclastics: Bull. Volcanol., v. 32-2, p. 303-317.

Ward, J. K., 1973, Geomorphic effects of pyroclastic volcanism: a determinïstic modeling approach: unpublished disertation, University of Iowa, 193 p.

Wentworth, C. K., and Williams, Howell, 1932, The classification and terminology of the pyroclastic rocks: Nat. Res. Council Rept. Comm. Sedimentation Bull., v. 89, p. 19-59.

Wilcox, R. E., 1959, Some effects of recent volcanic ashfalls with especial reference to Alaska: U.S. Geol. Survey Bull. 1028-N, p. 409-476.

APPENDIX 1

Explanation of the Munsell Soil Color System (quoted in part from the Munsell Soil Color Chart, 1973)

Colors are defined in the Munsell system by three variables which combine to describe all colors. These variables are called hue, value, and chroma and are defined as follows:

Hue - indication of the relation of a given color to red, yellow, green, blue, or purple

Value - indication of color lightness

Chroma - indication of strength or departure from a neutral color of the same lightness

"The nomenclature for all soil color consists of two complementary systems (1) color names, and (2) the Munsell notation of color. The color names are used in all descriptions for publication and for general use. The Munsell notation is used wherever greater precision is needed, as a convienient abbreviation for field descriptions, for expression of the specific relations between colors, and for the statistical treatment of color data."

"The Munsell notation for color consists of separate notations for hue, value, and chroma, which are combined in that order to form the color designation. The symbol

is the letter abbreviation of the color of the rainbow preceded by the number 0-10. Within each letter range, the hue becomes more yellow and less red as the numbers increase. The middle of the letter range is at 5; the zero point coincides with the 10 point of the next redder hue. Thus, 5YR is in the middle of the yellow-red hue, which extends from 10R to 10YR."

"The notation for value consists of number from 0, for absolute black, to 10 for absolute white. Thus a color value 5/ is visually midway between absolute black and absolute white."

"The notation for chroma consists of numbers beginning at 0 for neutral greys and increasing at equal intervals to a maximum of about 20. For absolute achromatic colors (pure greys, blacks, and whites) which have zero chroma and no hue, the letter N (neutral) takes the place of a chroma designation."

"In writing the Munsell notation, the order is hue, value, chroma with a space between the hue letter and succeeding value number, and a slash between the two numbers for value and chroma." For example, the notation of a color of hue 5R, value 3, and chroma 1, is 5R 3/1, a dark red-grey.

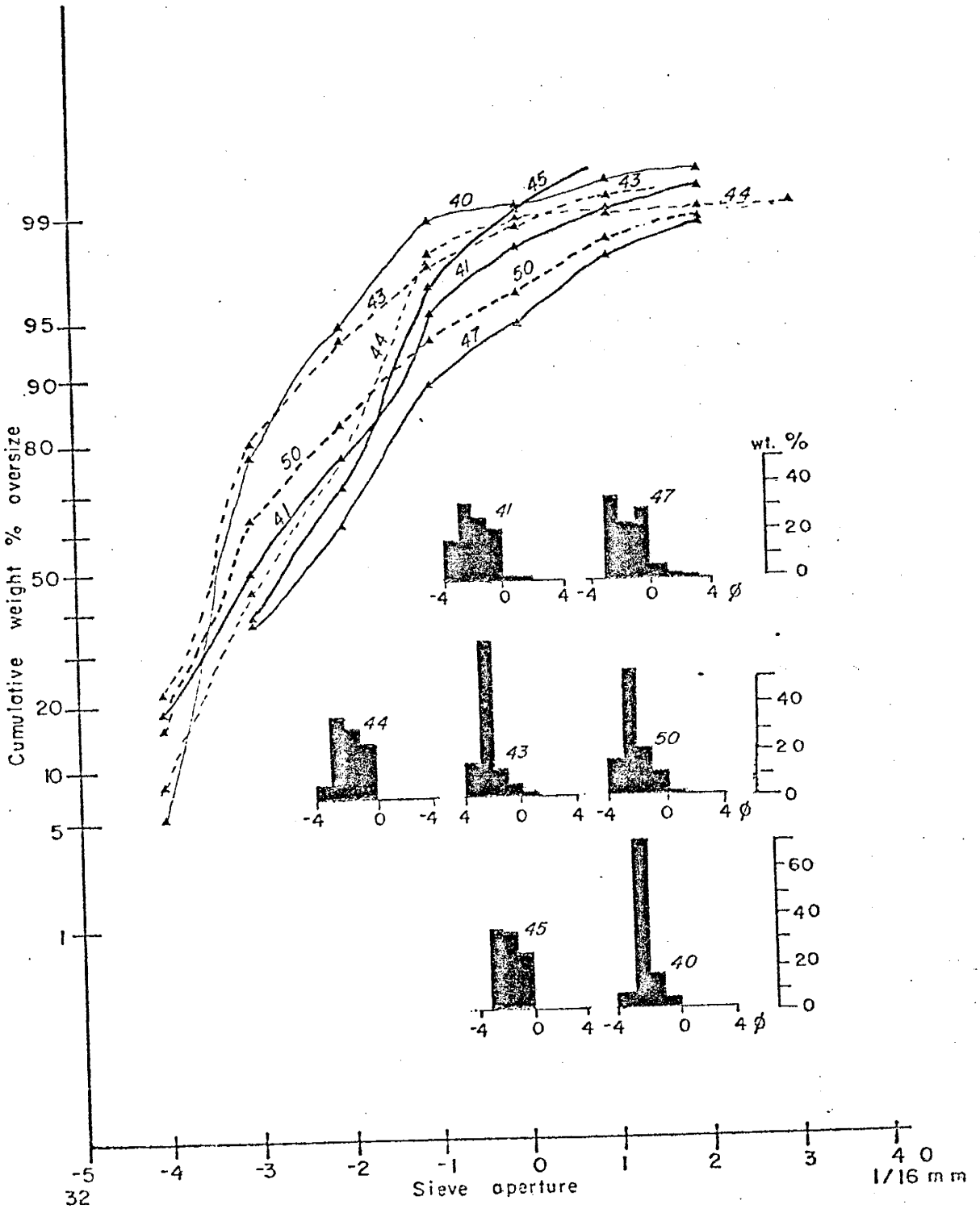

Appendix 2: Graphical representation of grain size characteristics showing histograms and cummulative curves.

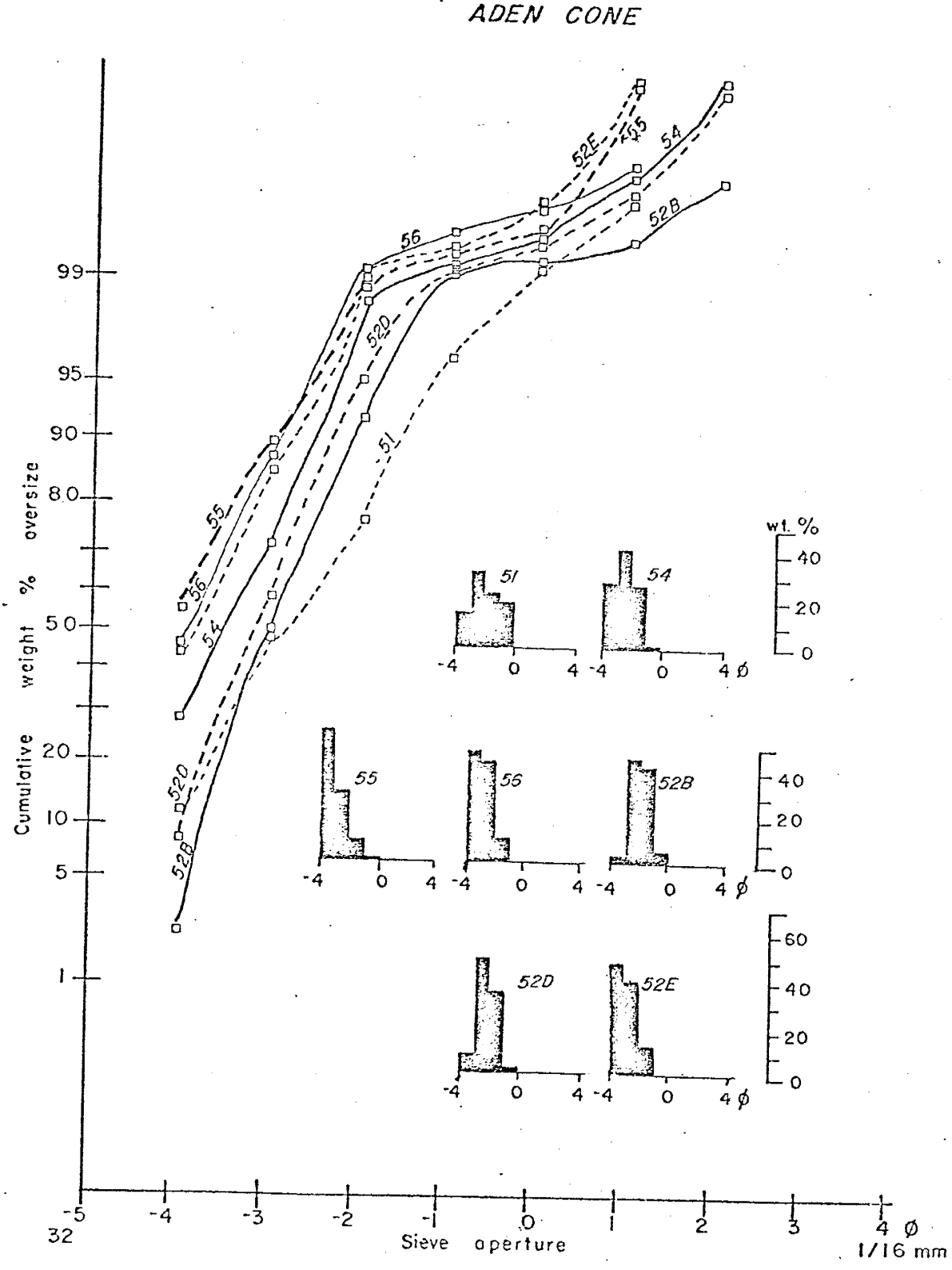
ADEN CONE
Cumulative weight % oversize
99
95
90
80
50
20
10
5
1
52E
405
54
56
52B
52D
51
55
56
54
52D
52B
51
54
55
56
52B
52D
52E
wt. %
40
20
0
60
-4
0
4
4 ø
-5
-4
-3
-2
-1
0
1
2
3
4 ø
32
Sieve aperture
1/16 mm

TWIN MOUNTAIN

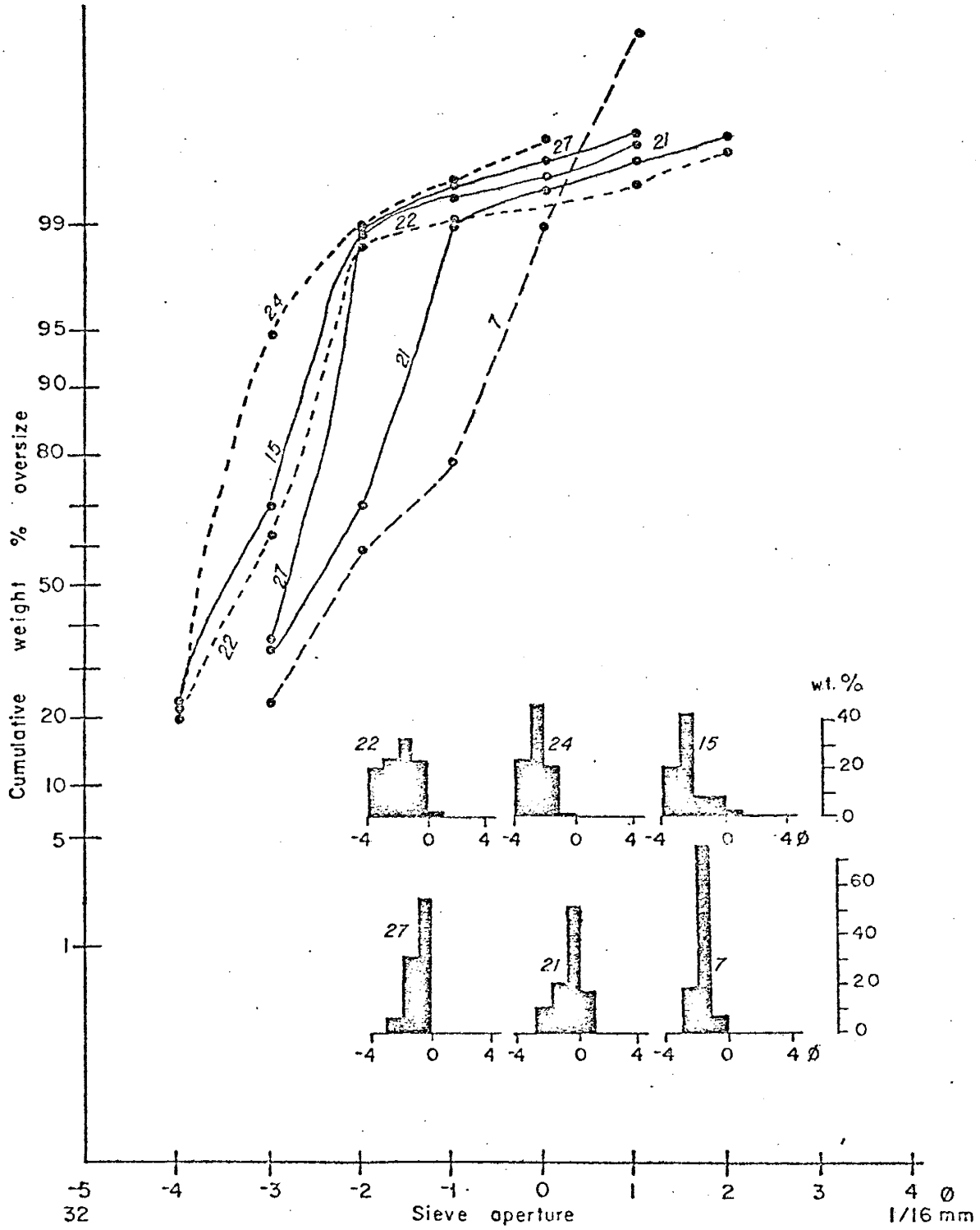

BLACKBIRD HILL

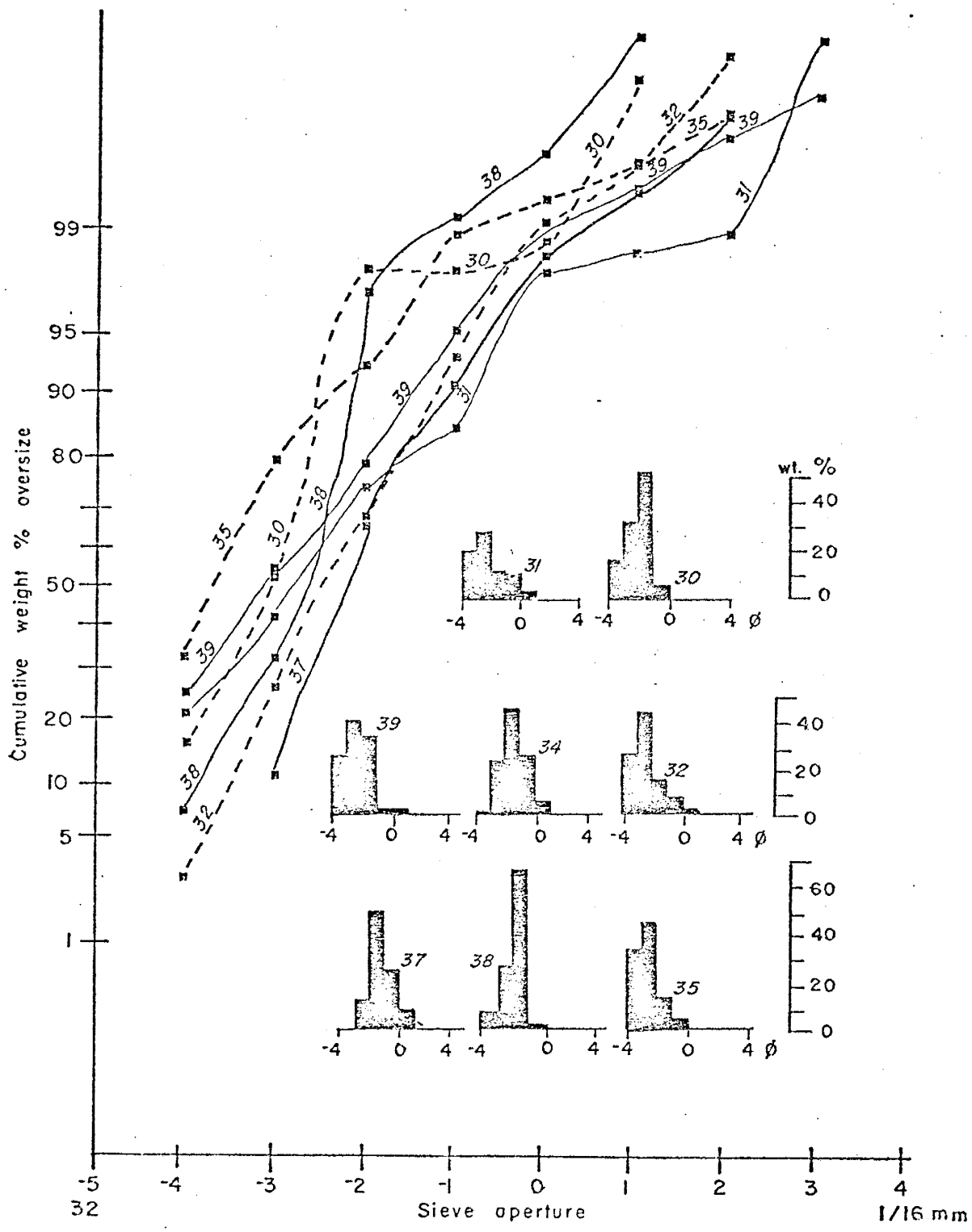

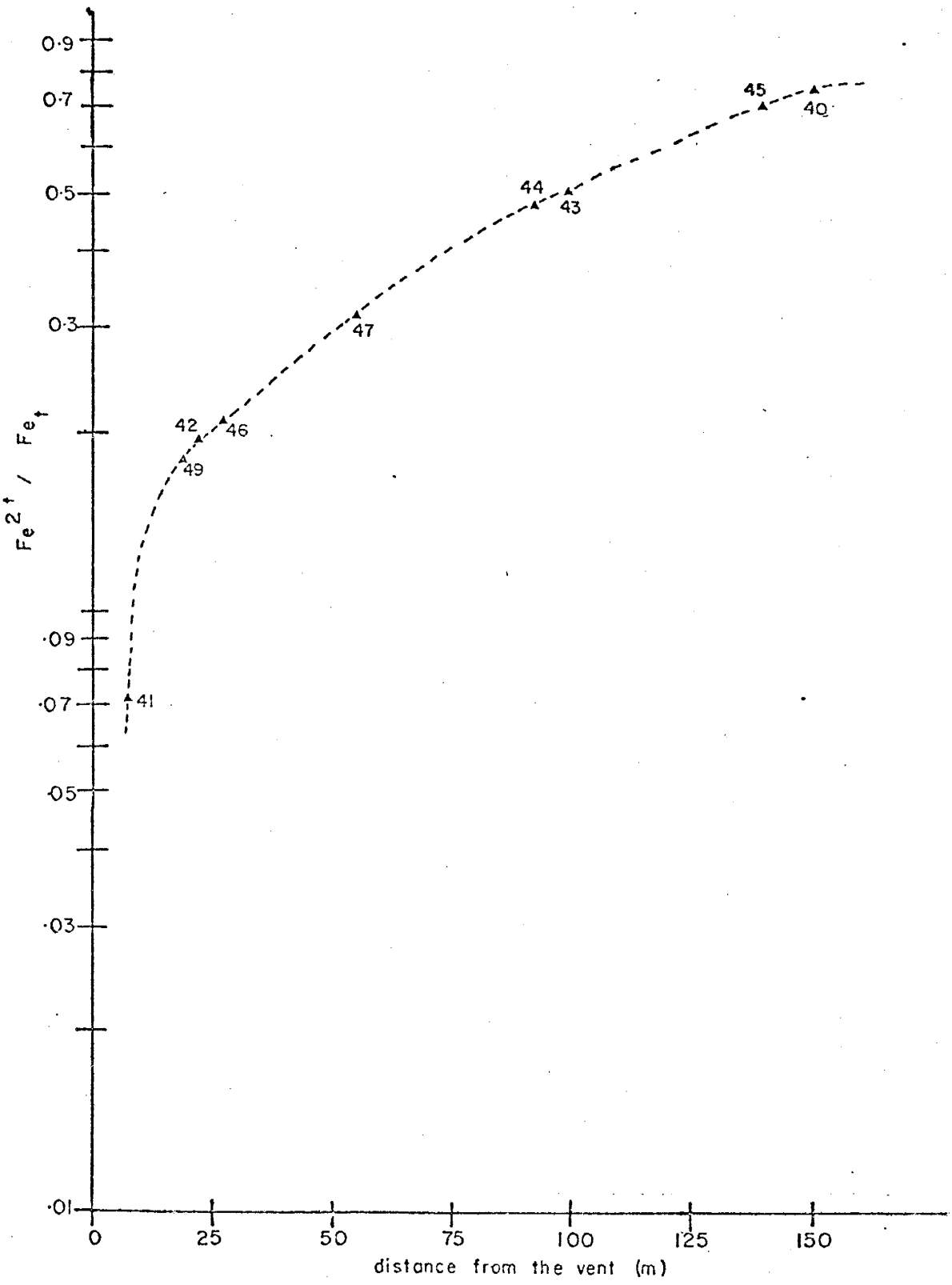

Appendix 3: Graphical presentation of variation of the oxidation state of iron against distance from the vent.

ADEN CONE

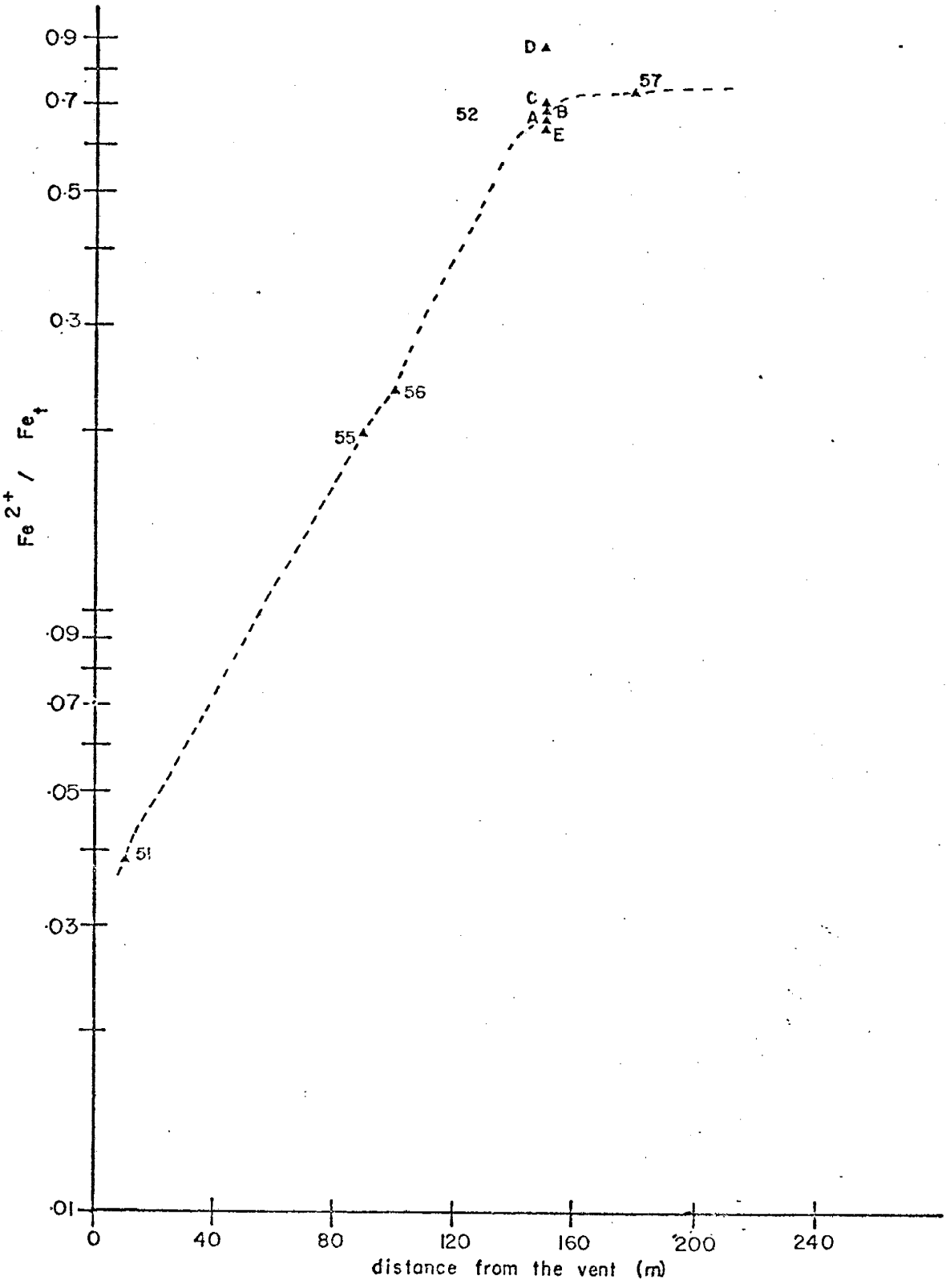
0·9
0·7
0·5
0·3
·09
·07
·05
·03
·01
Fe^{2+} / Fe_t
D
C
B
A
E
52
57
56
55
51
0
40
80
120
160
200
240
distance from the vent (m)

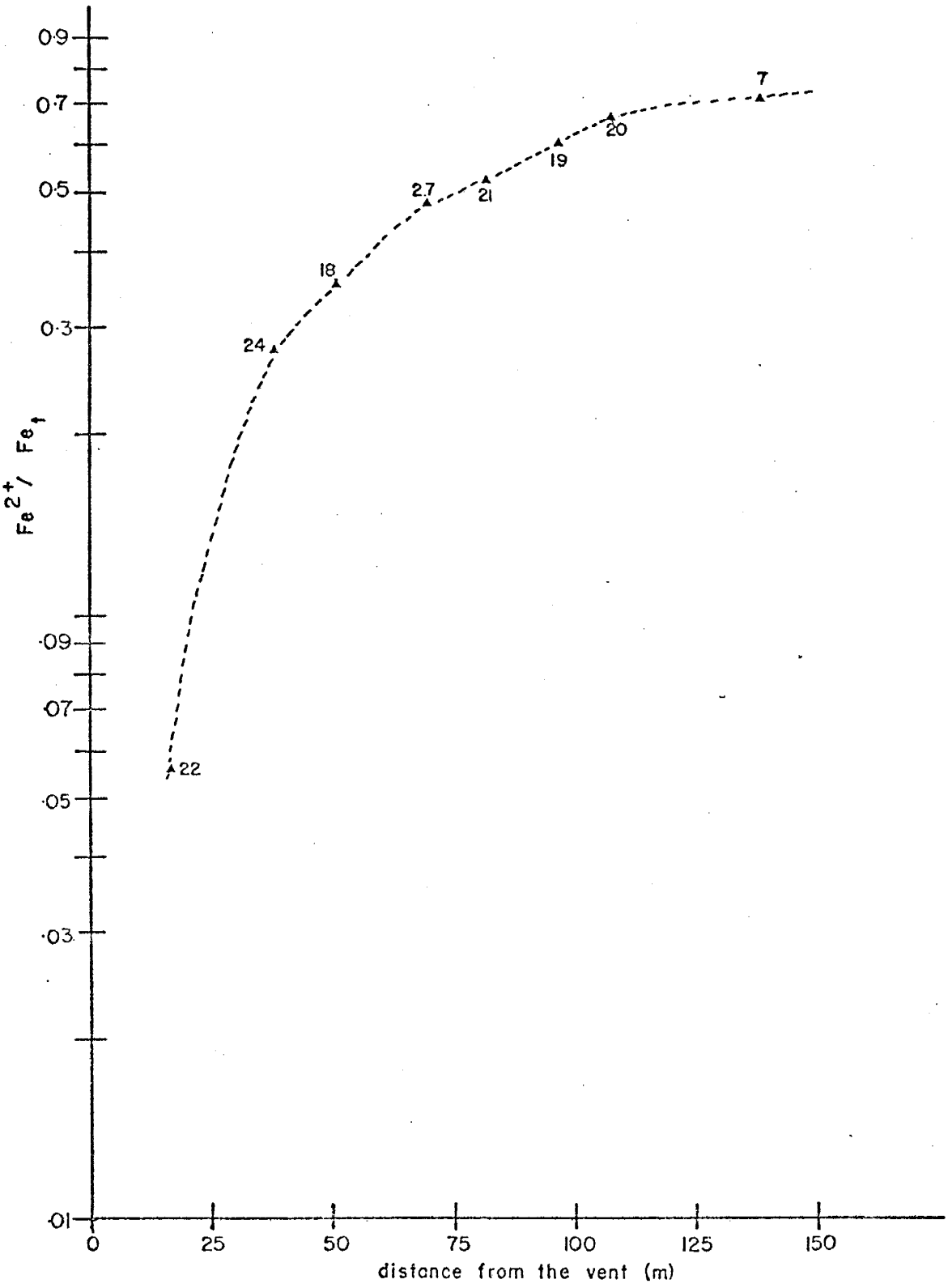
TWIN MOUNTAIN
0·9
0·7
0·5
0·3
·09
·07
·05
·03
·01
Fe^{2+}/Fe_t
0
25
50
75
100
125
150
distance from the vent (m)
7
20
19
27
21
18
24
22

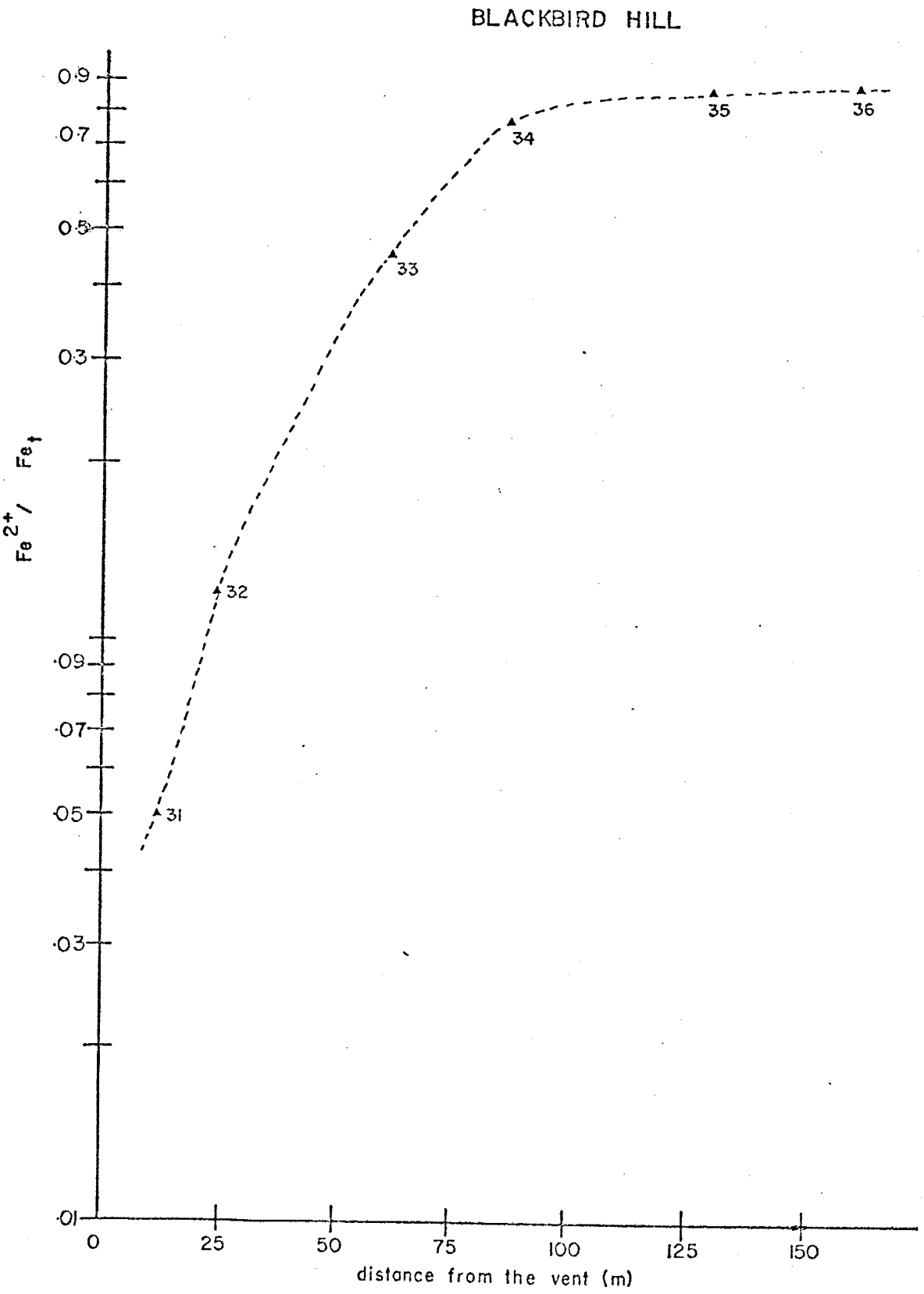
BLACKBIRD HILL
0·9
0·7
0·5
0·3
·09
·07
·05
·03
·01
Fe^{2+}/Fe_t
31
32
33
34
35
36
0
25
50
75
100
125
150
distance from the vent (m)

APPENDIX 4.

HEATING TEST DATA

SAMPLE	COLOR	T. (°C)	t. (hr.)	COLOR	t. (hr.)	COLOR	t. (hr.)	COLOR	t. (Hr.)	COLOR
18	dk red grey 10YR 3/1	400	12	dk red grey 10YR 3/1	24	dk red grey 5YR 4/2	42	dk red grey 5YR 4/2	84	dk red brown 5YR 3/2
19	v dk grey 2.5YR N3/	400	12	v dk grey 10YR 3/1	24	v dk grey 10YR 3/1	42	v dk grey 10YR 3/1	84	v dk grey 10YR 3/1
20	dk grey 2.5YR N4/	400	12	dk grey 10YR 4/1	24	dk grey 10YR 4/1	42	dk grey 10YR 4/1	84	dk grey 5YR 4/1
24	dk red brown 5YR 3/3	400	12	dk red grey 5YR 4/2	24	wk red 2.5YR 4/2	42	dk red grey 5YR 4/2	84	wk red 2.5YR 4/2
25	dk grey 7.5YR N4/	400	12	dk grey 10YR 4/1	24	dk brown 7.5YR 4/2	42	dk brown 10YR 4/2	84	dk brown 10YR 4/2
27	v dk grey 10YR 3/1	400	12	v dk grey 10YR 3/1	24	v dk grey 10YR 3/1	42	v dk grey 7.5YR N3/	84	v dk grey 7.5YR N3/
40	v dk grey 10YR 3/1	400	12	dk grey 10YR 4/1	24	dark grey 10YR 4/1	42	v dk grey br 10YR 3/2	84	v dk grey br 10YR 3/2
40s	v dk grey 2.5Y N3/	400	12	v dk grey 7.5YR N3/	24	v dk grey 7.5YR N3/	42	v dk grey 7.5YR N3/	84	dk grey 10YR 4/1
43s	v dk grey 2.5YR N3/	400	12	v dk grey 10YR 3/1	24	v dk grey 2.5YR N3/	42	v dk grey br 10YR 3/2	84	v dk grey br 10YR 3/2
44s	black 5Y 2.5/2	400	12	v dk grey 2.5Y N3/	24	v dk grey 2.5YR N3/	42	v dk grey 7.5YR N3/	84	dk olive 5Y 2.5/3
45	v dk grey br 10YR 3/2	400	12	brown 10YR 5/3	24	lt yel br 10YR 6/3	42	lt yel br 10YR 6/3	84	lt yel br 10YR 6/3
52A	v dk grey 2.5YR N3/	400	12	v dk grey br 10YR 3/2	24	dk grey br 10YR 4/2	42	dk grey red 5YR 4/2	84	wk red 10R 4/3
52Ds	v dk grey 2.5Y N3/	400	12	v dk grey br 2.5Y N3/	24	v dk grey 10YR 3/1	42	v dk grey 10YR 3/1	84	v dk grey 5YR 3/1
52Es	v dk grey 2.5YR N3/	400	12	v dk grey 10YR 3/1	24	v dk grey 10YR 3/1	42	v dk grey 5YR 3/1	84	dk red br 5YR 3/3
54s	v dk grey 2.5YR N3/	400	12	v dk grey 7.5YR N3/	24	v dk grey 7.5YR N3/	42	v dk grey 7.5YR N3/	84	v dk grey 2.5YR N3/

SAMPLE	$COLOR_I$	T. (°C)	t. (hr.)	COLOR	t. (hr.)	COLOR	t. (hr.)	COLOR	t. (hr.)	COLOR	t. (hr.)	COLOR
07s	v dk grey 10YR 3/1	700	1	v dk grey 7.5YR N3/	2	v dk grey 2.5YR N3/	3	v dk grey 2.5YR N3/	4	v dk grey 2.5YR N4/	8	v dk grey 2.5YR N3/
18	dk red grey 10Y 3/1	700	1	dk red grey 5YR 4/2	2	dk red brown 5YR 3/2	3	dk red brown 5YR 3/2	4	reddish br 5YR 3/3	8	wk red 2.5YR 4/2
19	v dk grey 5YR N3/	700	1	dk red brown 5YR 3/2	2	dk red brown 5YR 3/2	3	dk red brown 5YR 3/2	4	reddish br 5YR 4/2	8	dk red grey 5YR 4/2
24	dk red brown 5YR 3/3	700	1	wk red 2.5YR 4/2	2	wk red 2.5YR 4/2	3	wk red 2.5YR 4/2	4	wk red 2.5YR 4/2	8	wk red 2.5YR 4/2
25	dk grey 7.5YR N4/	700	1	dk red grey 5YR 4/2	2	wk red 2.5YR 4/2	3	wk red 2.5YR 4/2	4	wk red 2.5YR 4/2	8	wk red 2.5YR 4/2
25s	black 2.5Y 2/0	700	1	dk grey 7.5YR N4/	2	dk grey 5YR 4/1	3	dk grey 5YR 4/1	4	red brown 5YR 4/1	8	dk red grey 5YR 4/2
27s	v dk grey 7.5YR N3/	700	1	v dk grey 7.5YR N3/	2	v dk grey 7.5YR N3/	3	v dk grey 7.5YR N3/	4	dk red grey 2.5YR 4/1	8	dk red grey 5YR 4/2
43s	v dk grey 2.5YR 3/1	700	1	dk grey 5YR 4/1	2	dk grey 10YR 4/1	3	dk red br 5YR 3/2	4	wk red 2.5YR 4/2	8	wk red 2.5YR 4/2
44s	v dk grey 7.5YR N3/	700	1	dk grey 5YR 4/1	2	dk grey 10YR 4/1	3	dk grey 5YR 4/1	4	reddish br 5YR 5/4	8	dk red grey 5YR 4/2
45s	v dk grey 7.5YR N3/	700	1	dk grey 2.5YR N4/	2	dk grey 5YR 4/1	3	red brown 5YR 4/3	4	red brown 2.5YR 4/4	8	wk red 2.5YR 4/2
52Bs	v dk grey 2.5YR N3/	700	1	v dk grey 2.5YR N3/	2	dk grey 7.5YR 4/1	3	v dk grey 2.5YR N3/	4	dusky red 10R 3/2	8	wk red 2.5YR 4/2
52Es	v dk grey 2.5Y 2.5/1	700	1	v dk grey 2.5YR N3/	2	dk grey 2.5YR N3/	3	v dk grey 10R 3/1	4	dusky red 2.5YR 4/2	8	wk red 10R 4/2

This thesis is accepted on behalf of the faculty of the Institute by the following committee:

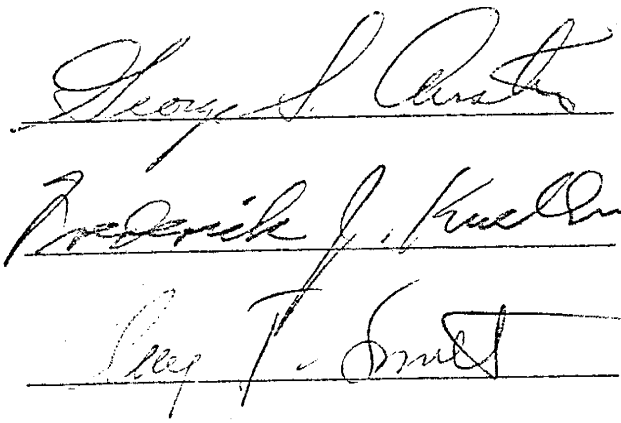

Date 11/27/78